Theoretical and Applied Climatology (2020) 140:69–89
https://doi.org/10.1007/s00704-019-03064-8

ORIGINAL PAPER

Investigation of seasonal droughts and related large-scale atmospheric dynamics over the Potwar Plateau of Pakistan

N. U. Ain[1] · M. Latif[1] · K. Ullah[1] · S. Adnan[2] · R. Ahmed[1] · M. Umar[1] · M. Azam[3,4]

Received: 23 May 2019 / Accepted: 25 November 2019 / Published online: 24 December 2019

Abstract

As a result of climate change and unsustainable land use management in the recent past, droughts have become one of the most devastating climatic hazards whose impacts may prolong from months to years. This study presents analysis of droughts for two major cropping seasons, i.e., Kharif (May–September) and Rabi (October–April), over the Potwar Plateau of Pakistan. The analysis is performed using various datasets viz. observational, reanalysis, and Regional Climate Models (RCMs), for the past (1981–2010) and future (2011–2100) time periods. The following two methods for the identification of dry and wet years, also referred to as drought and wetness, are applied: (1) the percentile rank approach and (2) the drought indices, Standardized Precipitation Index (SPI) and Reconnaissance Drought Index (RDI). Future projections of droughts are investigated using RCM (RegCM4.4 and RCA4) outputs from CORDEX South Asia domain under two Representative Concentration Pathway (RCP) scenarios, RCP4.5 and RCP8.5. Generally, the indices show non-significant decreasing trends of drought severity in the recent past for all cases; however, significant increasing trends are observed for annual (0.006) and Kharif (0.007) cases under RCP4.5 scenario. The analysis of large-scale atmospheric dynamics suggests the significant role of low-level geopotential height anomalies over Tibetan Plateau (northwest of Pakistan) during Kharif (Rabi) season in controlling drought occurrence by transporting moisture from the Bay of Bengal (Arabian Sea). Moreover, composites of vertically integrated moisture transport, moisture flux convergence/divergence, and precipitable water anomalies show their marked contribution in maintaining the drought/wetness conditions over the Potwar region.

1 Introduction

Drought is considered as the most severe and least understood natural hazard, resulting in prolonged dry period in natural climate cycle, that can have serious impacts on crop yield, environmental conservation, socioeconomic development, infrastructure, health, and Gross Domestic Product (GDP) of a country (Kao and Govindaraju 2010; Zargar et al. 2011; Hao and Aghakouchak 2014; Zhang et al. 2015; Ullah et al. 2017). It is broadly defined as an extended period of below-average precipitation, leading to a severe water shortage in an ecological system (Gonzalez-Hidalgo et al. 2009). Palmer (1968) defined drought as a meteorological phenomenon that severely affects an area and causes moisture deficiency. The drought can be categorized into the following three major types: meteorological, hydrological, and agricultural. According to Wilhite (2000), drought can occur anywhere in the world and in any climatic region (arid, semi-arid, or humid), but their spatio-temporal characteristics vary significantly among regions. The interannual fluctuations in precipitation often place the arid regions at higher drought risk due to greater likelihood of abnormally low precipitation (Le Houérou 1996; Smakhtin and Schipper 2008). Since most of Pakistan lies in an arid climate zone where droughts have been a recurring event (Haider and Adnan 2014), the study of historical droughts will help in the delineation of drought-prone areas, and thereby, contingency plans can be developed by the government authorities to cope with the hazardous effects of this natural disaster (Adnan et al. 2018).

✉ M. Latif
muhammad_latif@comsats.edu.pk

[1] Department of Meteorology, COMSATS University Islamabad (CUI), Islamabad 45550, Pakistan

[2] Pakistan Meteorological Department (PMD), National Drought Monitoring Centre, Islamabad 44000, Pakistan

[3] Faculty of Agricultural Engineering and Technology, PMAS Arid Agriculture University, Rawalpindi 44000, Pakistan

[4] Postdoctoral Research Associate, Chungbuk National University, Chungcheongbuk-do, South Korea

Owing to the socio-economic effects of droughts, many studies have been carried out across different regions of the world, and different indices and techniques have been employed to monitor the frequency, duration, and severity of drought (Zhang and Zhou 2015; Tabari et al. 2012; Pietzsch and Bissolli 2011). According to Mendicino et al. (2008), drought indices are reliable and useful tools for monitoring and forecasting drought conditions. Hisdal et al. (2001) studied the hydrological droughts using threshold-level approach and found that the variability in precipitation can explain the trends of drought occurrence, frequency, and duration. Narasimhan and Srinivasan (2005) developed two drought indices, Soil Moisture Deficit Index (SMDI) and the Evapotranspiration Deficit Index (ETDI), for the monitoring of agricultural drought using the Soil and Water Assessment Tool (SWAT) model. Adnan et al. (2018) applied different drought indices and reported that, among 15 different indices used, the Standardized Precipitation Index (SPI) (McKee et al. 1993), Standardized Precipitation Evapotranspiration Index (SPEI) (Vicente-Serrano et al. 2010), and Reconnaissance Drought Index (RDI) (Tsakiris and Vangelis 2005; Tsakiris et al. 2007) perform well in assessing drought conditions over Pakistan and adjacent areas. Other common drought indices that are being used extensively by the national hydro-meteorological organizations include the Palmer Drought Severity Index (PDSI) (Palmer 1965), Deciles Index (DI) (Gibbs and Maher 1967), China Z Index (CZI) (Wu et al. 2001), Crop Moisture Index (CMI) (Palmer 1968), and Surface Water Supply Index (SWSI) (Shafer and Dezman 1982).

Pakistan is ranked on the seventh position among the most affected countries by the impacts of extreme weather events during 1996 to 2015 (Kreft et al. 2013). Variability of droughts in Pakistan has captured the attention of many researchers in the recent past. Pasha et al. (2015) studied droughts over the Sindh Province of Pakistan and showed that human-induced warming has increased drought risk in the country. Adnan et al. (2018) evaluated the performance and efficiency of various drought indices over Pakistan using the data of 58 meteorological stations for the period 1951–2014. Their results obtained by most of the indices showed significantly increasing (towards wetness) trends. Adnan and Haider (2012) studied the classification and assessment of aridity in Pakistan for the period 1960–2009 and reported that the southern parts of the country are more vulnerable to drought conditions compared with the northern areas. The southern parts of Pakistan have also been identified as the most drought-vulnerable region by Anjum et al. (2010). Haroon et al. (2016) employed MODIS-based Drought Severity Index (DSI) to investigate drought conditions in Pakistan and found severe drought during 1998–2002 in the region. Their results further revealed that the MODIS-Terra NDVI values can be used as a tool to identify wet and dry conditions in large-scale studies; however, the technique is not suitable for regional scale studies, as it is hard to detect drought signal just from NDVI anomaly values alone. Adnan et al. (2016) conducted drought analysis on monthly, annual, and decadal time-scales using different indices during 1951 to 2010 in the South Central Asia (SCA) region, with particular focus on Pakistan. They found two major drought periods, i.e., 1971 and 2000–02, where 2001 was reported as an extremely dry year in the SCA region. The drought onset, end, and severity are difficult to predict, and it still poses a challenge, especially over the rainfed region of Potwar Plateau, which needs to be addressed to get a more insight on this costly natural event.

The Potwar Plateau of Pakistan (PPP) lies in the dominant precipitation region of Pakistan (see, for instance, Latif and Syed 2016; Latif et al. 2017), which receives precipitation not only during summer season but also in winter through southwest monsoon and western disturbance weather systems, respectively. Agricultural productivity of PPP relies heavily on adequate water supply, which depends solely on the timely rainfall (Rashid and Rasul 2011). A slight variability in the rainfall and water stress at any crop phonological stage can affect the grain yield (Cakir 2004). Although many studies (e.g., Sajjad and Ghaffar 2018; Ahmad and Hussain 2017; Ali et al. 2016) have investigated climatic extremes related to temperature and precipitation in Pakistan, drought assessment and its related large-scale atmospheric dynamics as well as the future projections using Regional Climate Model (RCM) simulations for major cropping seasons have not been studied over the PPP. In this study, we aim to fill the above-mentioned gaps by investigating the past and future drought as well as related dynamics in the Potwar Plateau.

The structures of the paper are organized as follows: Study area, data, and methods are described in Section 2. The results and discussions are presented in Section 3, which include the analysis of drought frequency, severity, and trends; large-scale dynamics associated with extremely dry/wet cases; and future drought projections using RCMs. Finally, the summary and conclusions of this study are presented in Section 4.

2 Data and methods

2.1 Study area

The Potwar Plateau (32.5°–34°N and 72°–74°E) is located in the north-east Pakistan with a total area of about 5000 miles^2 (Fig. 1). The Potwar region includes four districts—Jhelum, Chakwal, Rawalpindi, and Attock—and Islamabad, the capital territory (Rashid and Rasul 2011). The climate of most of the area is semi-arid to humid with annual rainfall ranging from 900 to 1900 mm (Adnan et al. 2009; Adnan and Khan 2009). Generally, two major weather systems, i.e., southwest monsoon (Latif and Syed 2016) and western disturbances (Ahmed et al. 2019a, b; Hussain and Lee 2009), cause rainfall over the PPP

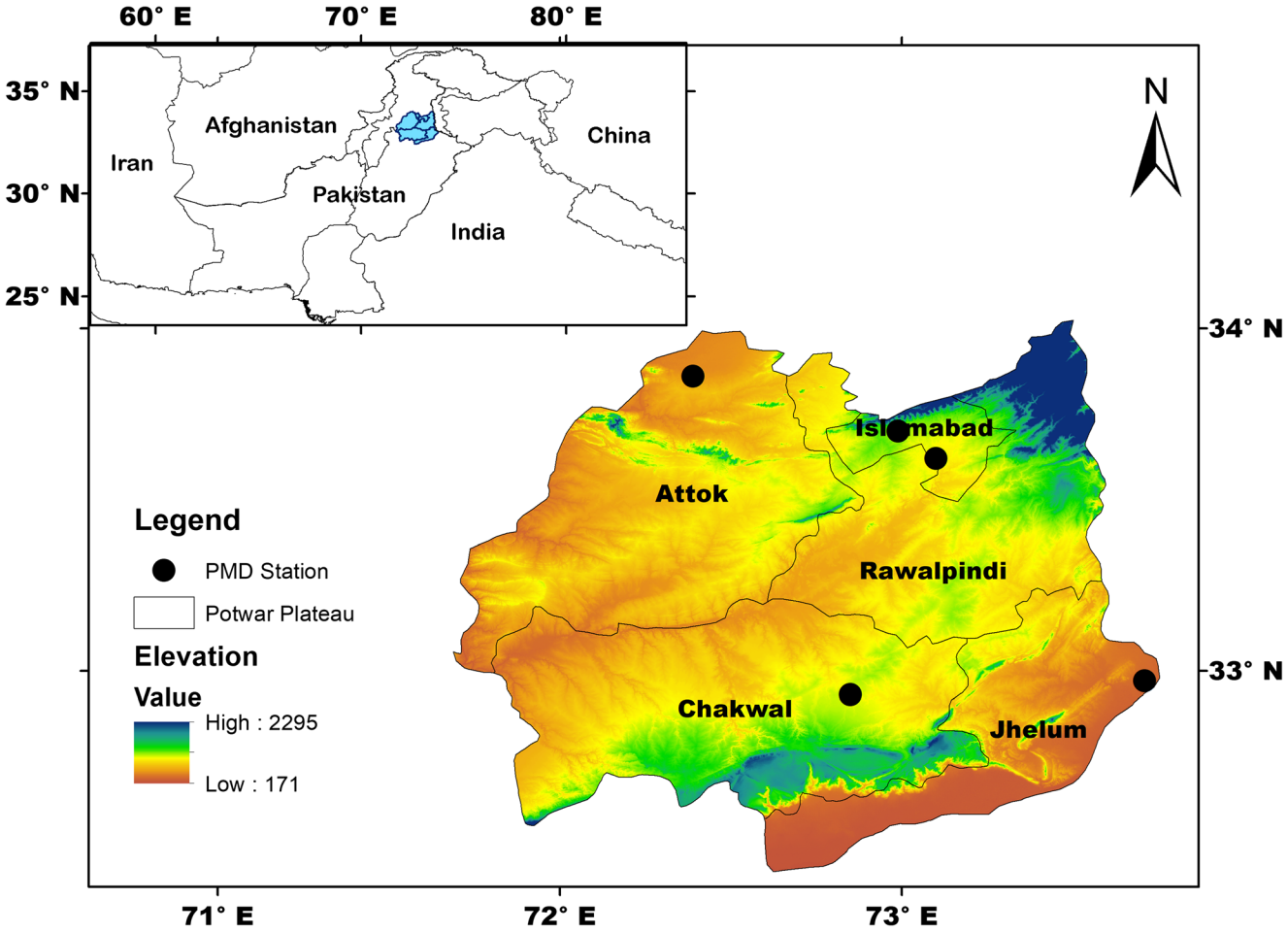

Fig. 1 Study area map of Potwar Plateau of Pakistan. Black circles show the location of PMD stations, whereas the shading represents the elevation in meters

during the summer (July–September) and winter (December–March) seasons, respectively. The mean annual maximum and minimum temperature ranges between 26 °C and 13 °C, respectively (Adnan et al. 2017). Kharif (May–September) and Rabi (October–April) are the two major crop growing seasons in the PPP. The spatial distribution pattern of the mean seasonal (cropping seasons) and annual precipitation and temperature over Pakistan is shown in Fig. 2. The sowing and harvesting time of Kharif crops (rice, maize, cotton, soybean, jowar, moong, ground nut, etc.) are May–June and October–November, whereas Rabi crops (wheat, onion, tomato, potato, mustard, carrot, oat, isabgol, barley, etc.) are usually sown during November–December and harvested in March–April. The crop yield of the PPP contributes to about 10% of the total agriculture production (Ashraf 2004). The summer monsoon rainfall alleviates moisture stress conditions during the Kharif season and fulfills the water requirements for Rabi crops (Adnan et al. 2018). The spatio-temporal variability of precipitation during both seasons can affect negatively the GDP of the country, as agriculture sector accounts for about 24% of GDP alone (Latif and Syed 2016; IUCN 2009).

2.2 Observed and reanalysis datasets

In order to examine drought conditions over the PPP in the past three decades (1981–2010), six monthly observational temperature and precipitation datasets at 0.5 × 0.5° horizontal resolution are used in this study. These datasets are obtained from the following different sources: (1) Climate Data Processing Centre (CDPC), Pakistan Meteorological Department (PMD); (2) Global Precipitation Climatology Centre (GPCC) V6 (Schneider et al. 2015); (3) University of East Anglia, UK Climatic Research Unit (CRU) TSv.4.01 (Harris et al. 2014); (4) Asian Precipitation-Highly Resolved Observational Data Integration Towards Evaluation of Water Resources (APHRODITE) V1101 (Yatagai et al. 2012) by Research Institute for Humanity and Nature (RIHN) and Meteorological Research Institute of Japan Meteorological Agency; (5) University of Delaware (UDEL) global gridded high-resolution station (land) data (Willmott and Matsuura 2005); and (6) NAA Precipitation Reconstruction over Land (PREC/L) (Chen et al. 2002). Era-interim reanalysis data product (Ma et al. 2018) by the European Center for Medium-range Weather Forecast

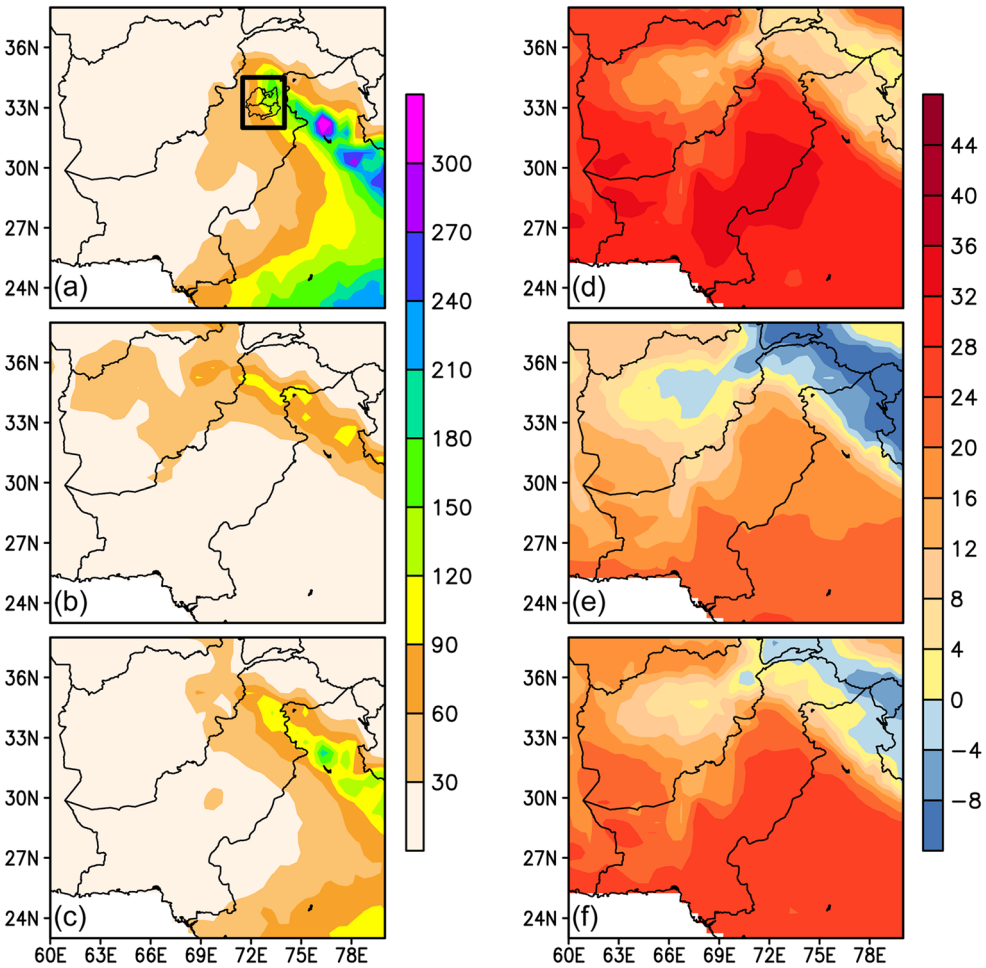

Fig. 2 Left panels (**a**–**c**): precipitation climatology (units: mm/month) during Kharif, Rabi, and annual time-scales, respectively, for the period (1981–2010) using GPCC gridded datasets. Right panels (**d**–**f**): same as left panels except for temperature (units: °C) using CRU datasets. Rectangular boxed region in panel a shows the study region

(ECMWF) is also used to check for consistency with station and observed datasets.

In order to study the large-scale circulation anomalies associated with Extremely Dry (ED) and Extremely Wet (EW) events, also referred as drought and wetness conditions, NCEP (National Center for Environmental prediction)/NCAR (National Center for Atmospheric Research) reanalysis data of geopotential height, u & v winds, and vertical velocity (ω) with 2.5° × 2.5° spatial resolution (Kalnay et al. 1996) are used.

2.3 Model datasets

The fourth version of the Rossby Centre regional atmospheric model (RCA4) at the Swedish Meteorological and Hydrological Institute (SMHI) and RegCM4.4 at the Abdus Salam International Center for Theoretical Physics (ICTP) RCM outputs with different Global Climate Models (GCMs) as Lateral Boundary Conditions (LBCs) are obtained from COordinated Regional climate Downscaling EXperiment (CORDEX) framework for South Asian domain with 0.44° × 0.44° (approximately 50 × 50 km grid spacing) horizontal resolution (Table 1). The CORDEX experiment is developed by the World Climate Research Program (WCRP) which aims to produce high-resolution regional climate projections for the future climatic analysis at regional scale (Giorgi et al. 2009). RCM simulations with ERA-Interim as LBCs (Dee et al. 2011) are used for model evaluation of the recent past climate. The historical simulations (1961–2005) are based on the assumption of anthropogenic gas emission and aerosol ejection into the atmosphere (Latif et al. 2018). Whereas, future (2006–2100) simulations are based on two Representative Concentration Pathway (RCP) scenarios (Moss et al. 2008), i.e., RCP4.5: medium-to-high CO_2 emission scenario and RCP8.5: high CO_2 emission scenario. In this study, we used both RCP4.5 and RCP8.5 scenarios which represent the categories of "medium" and "high" greenhouse gas emission scenarios, respectively, and prescribe the future radiative forcing level of 4.5 and 8.5 W/m^2, respectively, by the end of the twenty-first century.

2.4 Methodology

The performance of observational temperature and precipitation gridded datasets is evaluated first for both Kharif and Rabi seasons as well as on annual time-scales using the Taylor

Table 1 List of CORDEX South Asia regional climate model (RCM) experiments

No.	RCM description	Driving GCM	Name used	Model center	Historical and future
1	The Regional Climate Model system RegCM version 4. (RegCM4.4: Giorgi et al. (2012))	CCCMA-CanESM2	RegCM4.4	The Abdus Salam International Centre for Theoretical Physics (ICTP), Italy. CCCR, IITM, India	1951–2005 and 2006–2100
		CNRM-CM5			
		CSIRO-MK3-6-0			
		IPSL-CM5A-LR			
		MPI-ESM-MR			
		GFDL-ESM2M			
		ECMWF-ERAINT			1979–2008
2	Rossby Centre Regional Atmospheric Model version 4 (RCA4: Samuelsson et al. (2011))	CCCMA-CanESM2	RCA4	Sveriges Meteorologiska Och Hydrologiska Institute (SMHI), Sweden.	1951–2005 and 2006–2100
		CNRM-CM5			
		CSIRO-MK3-6-0			
		EC-EARTH			
		IPSL-CM5A-MR			
		MIROC5			
		HadGEM2-ES			
		MPI-ESM-LR			
		NorESM1-M			
		GFDL-ESM2M			
		ECMWF-ERAINT			1980–2010

diagram (Taylor 2001). A Taylor diagram can provide concise statistical comparison between observed or reanalysis field and reference data in terms of analyzing the ratio of their variances, correlation coefficient, and root-mean-square difference. The best performing observed data is then used to check for consistency with station data for the study of droughts over the region. The percentile grading criteria is employed by averaging the monthly precipitation of all five meteorological stations that lie in the Potwar region (Fig. 1), to identify the EW and ED cases for both cropping seasons for the study period.

The percentile rank approach is given and calculated as:

$$R = \frac{P}{100(N+1)} \quad (1)$$

Where R is the rank order, percentile rank is represented by P, and N is the total number of values in the distribution.

We further applied two drought indices viz. SPI and RDI, to categorize the drought severity and also to check for consistency with the EW/ED cases as identified using percentile rank approach. SPI is calculated at different 3-, 6-, 9-, and 12-month aggregation time-scales. RDI is based on cumulative values of both precipitation and potential evapotranspiration (PET), where the values range between 1.5 to 3.0 and − 1.5 to − 3.0, which represent the EW and ED conditions, respectively. The percentile grading, SPI, and RDI criteria are given in Table 2.

The composite-anomaly patterns of geopotential height and winds (850 hPa), vertical velocity (500 hPa), precipitable water, vertically integrated (surface to 300 hPa) moisture transport (see, for instance, Latif et al. 2018 and Latif et al. 2017), and integrated moisture flux convergence/divergence (Ullah and Shouting 2012) are presented to study the large-scale atmospheric dynamics associated with EW and ED cases. Monthly anomalies are calculated by subtracting climatological monthly means from the data.

To study the future drought conditions over the PPP, the RegCM4.4 and RCA4 precipitation simulations, with Era-Interim and different GCMs as LBCs (Table 1), are compared with reference (station) data for selecting the best model for the analysis. The period 1981–2005 is used as the baseline (reference) period for model evaluation, whereas the time slice 2006–2100 is used for the future under RCP4.5 and RCP8.5 scenarios. RCM simulations driven by ERA-Interim as LBCs are used for assessing the model performance in the recent past climate. A non-parametric statistical test, Sen's slope estimator (Sen 1968), is used to identify the trend in drought indices (SPI and RDI), whereas Mann-Kendall test (Mann 1945; Kendall 1975; Gilbert 1987) is employed to ascertain the presence of statistical significance (5% significance level) of the trend in the time series.

3 Results and discussions

3.1 Performance of observed and reanalysis datasets

The pattern statistics between reanalysis/observed and PMD rain-gauge measurements for the normalized mean (1981–

Table 2 The wet and dry classes and grades based on percentile score (Kant et al. 2014), SPI, and RDI (Adnan et al. 2015) criteria

Percentile score			SPI and RDI		
Classes	Grades	Score (percentile)	Classes	Grades	Criteria
Extremely dry	ED	10 > ED > 0	Extremely dry	ED	− 2.0 or less
Large deficit	LD	20 > LD > 10	Severe dry	SD	− 1.50 to − 1.99
Moderate deficit	MD	30 > MD > 20	Moderate dry	MD	− 1.49 to − 1.00
Mild deficit	MID	40 > MID > 30	Normal	N	− 0.99 to 0.99
Normal	N	60 > *N* > 40	Moderate wet	MW	1.00 to 1.49
Mild excess	MIE	70 > MIE > 60	Severe wet	SW	1.50 to 1.99
Moderate excess	ME	80 > ME > 70	Extremely wet	EW	2.0 or more
Large excess	LE	90 > LE > 80			
Extremely wet	EW	EW > 90			

2010) precipitation and temperature for seasonal (Kharif and Rabi) and annual time-scales over the PPP is presented in the Taylor diagram (Fig. 3). The PMD station data are used as the reference dataset to evaluate the performance of reanalysis (Era-Interim) and observed (GPCC, CRU, APHRODITE, UDEL, and Precip/L) datasets over the study area. Taylor diagram shows 2-D plot based on three statistical parameters, i.e., Root Mean Square Error (RMSE), standard deviation (amplitude of the variations), and correlation coefficient. These parameters provide the best possible evaluation results for the selection of appropriate datasets. Based on the statistical comparison between six observational/reanalysis and station datasets, our results show that the GPCC and CRU (for precipitation) and APHRODITE (for temperature) approximate well with the station datasets during both Kharif and Rabi seasons. It is also noted that the Era-interim reanalysis does not perform well for both precipitation (Fig. 3a–c) and temperature (Fig. 3d–f) cases. The correlation of GPCC (CRU) precipitation (temperature) lies between 0.9 and 0.95, with smaller RMSE. For temperature, although APHRODITE seems more realistic and suitable (the correlation is above 0.9, standard deviation is near to reference line with small RMSE) for the analysis, the dataset is not used for further analysis due to the limited time period constraint. Ahmed et al. (2019a, b) tested the performance of four widely used gauged-based gridded precipitation datasets in the semi-arid, arid, and hyper-arid regions of Balochistan Province of Pakistan and reported that the GPCC performs much better compared with other gridded datasets. Cheema and Hanif (2013) also evaluated the performance of GPCC datasets over the Punjab Province of Pakistan and found strong correlation ($R^2 = 0.93$) with in-situ area-weighted precipitation. Our results regarding the performance of GPCC are in good agreement with previous findings; we have therefore chosen the GPCC in this study to check for consistency with the station (reference) data.

By employing percentile score, SPI, and RDI criteria (Table 2) and assigning different grades, we found that frequency of classes differs significantly between EW and ED years (Table 3). It is observed that SPI-based cases of precipitation deficit and surplus are almost equal in Kharif (5 dry and 5 wet) and Rabi (3 dry and 4 wet) seasons; however, surplus cases on annual time scale are slightly higher than deficit (3 dry and 5 wet). The results of RDI show that the deficit cases in Kharif are higher than surplus (4 dry and 3 wet), whereas the deficit cases are higher in Rabi compared with Kharif (5 dry and 4 wet).

On annual basis, RDI shows higher number of deficit cases than surplus (5 dry and 3 wet). The seasonal (Kharif and Rabi) and annual analyses also identify extreme surplus and deficit cases, which have been used in Section 3.3 to see if these can explain the possible linkage with the large-scale dynamics.

3.2 Analysis of drought intensity and trends

The percentile (10th and 90th) rank approach and two drought indices, i.e., SPI and RDI, are used to determine the ED and EW cases over the PPP during 1981–2010 for both seasonal (Rabi and Kharif) and annual bases (Fig. 4). The percentiles are calculated both for PMD station data as well as GPCC gridded precipitation data. This approach is quite useful, and therefore, it is being used widely by many researchers to bifurcate the dry and wet cases over different parts of the world (Hao et al. 2016; Raible et al. 2017; Sajjad and Ghaffar 2018). In Fig. 4, the driest cases (at 10th percentile) are observed in years 1986, 1987, 2002, and 2009, whereas the wet cases at 90th percentile are noted during 1987, 1994, and 1997. As discussed earlier, SPI and RDI are the two renowned drought indices that have been used for identifying the drought intensity as well as for the consistency measures with percentile method over the same period (1981–2010). The choice of an appropriate drought index is critical for the effective monitoring of drought over the region. To study the drought over Pakistan, Adnan et al. (2018) recommended SPI and RDI as the best performing drought indices over the country. Both of the indices are highly correlated to each other as well as with percentile for both PMD station and GPCC gridded datasets.

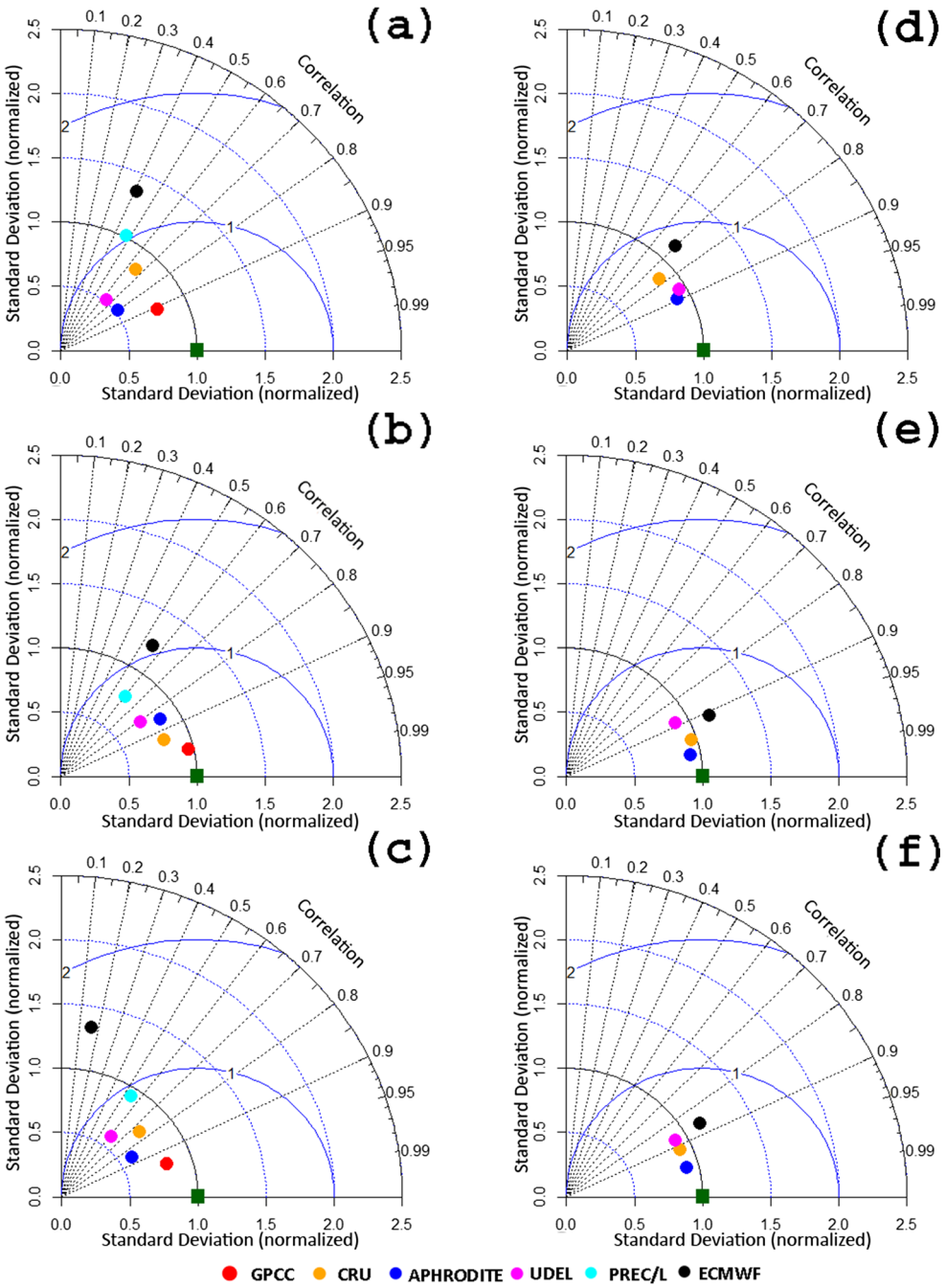

Fig. 3 Left panels (**a**–**c**): Taylor diagram representing a statistical comparison of gridded observed/reanalysis precipitation (units: mm/month) datasets with PMD station data for Kharif, Rabi, and annual time-scales, respectively, for the period (1981–2010). Right panels (**d**–**f**): same as left panels except for temperature

High interannual variability of the two drought indices has been observed for both Kharif and Rabi seasons, which may be attributed to the high interannual variability in the mean rainfall during summer (monsoon) or winter (western disturbances) seasons. The deficiency in seasonal rainfall may result in a drought situation over the PPP. It is also observed that the SPI index shows a positive slope (0.008) on both seasonal and annual time-scales for GPCC datasets (Fig. 4a,b), whereas negative (positive) is observed in Kharif (Rabi) season for station data. Moreover, the slope of RDI is positive (0.002) for Kharif and negative for both Rabi (− 0.010) and annual (− 0.009) bases. The positive and negative slopes of SPI and RDI drought indices represent wetter and drier episodes over the Potwar region.

SPI is further calculated at 3-, 6-, 9-, and 12-month aggregation time-scales on seasonal (Kharif and Rabi) and annual bases (Fig. 5). Drought intensity usually increases with increasing time-scales; therefore, an intense drought may not be determined on shorter timescale. Furthermore, SPI 3 is considered the most appropriate for short-term rainfall deficit or surplus cases, SPI 6 and SPI 9 are suitable for the monitoring of meteorological and agricultural droughts, and SPI 12 is

more effective for water resource management (Pashiardis and Michaelides 2008; Raziei et al. 2009; Adnan et al. 2015). High interannual variability of SPI is again observed during Kharif, Rabi, and annual basis; however, the Kharif season experiences the highest drought intensity (Fig. 5a). The negative slope of SPI on both seasonal and annual time-scales clearly indicates the decreasing trends (towards drought conditions). Due to the high intra-seasonal rainfall variability of PPP and its unique geographical location (receives highest amount of rainfall both in summer (Kharif) and winter (Rabi) seasons), drought period usually remains for a shorter time period and less intense as compared with other parts of the country. Since the Potwar region lies in the core precipitation zone of Pakistan, the drought or wetness events could be linked with the large-scale atmospheric dynamics to see if any physical linkages can be established.

3.3 Drought large-scale dynamics

In this section, the large-scale atmospheric dynamics for EW and ED cases over the PPP are presented for both Kharif and Rabi cropping seasons, as well as on annual time-scale as follows:

3.3.1 Geopotential height and wind anomalies

Composites of geopotential height and wind anomalies in the lower troposphere (850 hPa) for EW cases on seasonal (Kharif and Rabi) and annual time scales are shown in Fig. 6a–c. It is observed from Fig. 6a that a strong positive height anomaly (> 6 m) is located over the Tibetan plateau during EW-Kharif season. As a result of this anticyclone (positive height anomaly), a strong convergence zone is developed along the foothills of Himalayas. This convergence zone plays a significant role in transporting lower-level moisture-laden winds to blow from Bay of Bengal towards Pakistan, causing rainfall during the EW-Kharif season over the PPP. Another positive height anomaly (5 m) over north and a weak negative anomaly (< 1 m) over the south of Pakistan together act as positive feedback to strengthen the northward flow. It should also be noted that the PPP is dominated by the southwest summer monsoon season during Kharif cropping months. During EW-Rabi season (Fig. 6b), a strong east-west-elongated negative height anomaly (<− 6 m) (cyclone) is noticed over the southwest of Pakistan, north-east Arabian Sea, Kathiyawar Peninsula, and north-west India. This negative height anomaly, associated with the eastward moving westerlies, is mainly responsible for transporting moisture from the Arabian Sea branch to the PPP during EW-Rabi season. We may conclude that during the EW-Kharif (EW-Rabi) season, Tibetan anticyclone (westerly flow) plays a crucial role in moisture incursion from the Bay of Bengal (Arabian Sea) for wet conditions over the study region. The positive and negative patterns of height anomalies can also be seen on annual time-scale (Fig. 6c).

The geopotential height and wind composite anomalies for ED cases on seasonal and annual time scales are shown in Fig. 6d–f. The results are the same as for ED cases, but with a reverse sign of anomalies. The outflow of winds from the PPP is observed during Kharif (Rabi) season caused by the strong positive (negative) height anomalies over most of the region (Fig. 6d,e). An outward flow of winds from the Indo-Pakistan subcontinent, during ED-Kharif/Rabi cases, is mainly responsible for dry condition over the region, which can also be seen on annual time scale (Fig. 6f).

3.3.2 Moisture transport and moisture flux convergence/divergence anomalies

Results of the composite anomalies of Vertically Integrated Moisture Transport (VIMT) and moisture flux convergence/divergence for EW cases on seasonal (Kharif and Rabi) and annual time-scales are presented in Fig. 7a–c. The integrated moisture transport (surface–300 hPa) from the NCEP/NCAR reanalysis is calculated by integrating moisture fluxes from the pressure level data. In Fig. 7a, it is observed that the strong moisture flux convergence zones (negative anomalies; <− 2 kg m^{-2} s^{-1}) during the EW-Kharif season are located over the central Pakistan, along the southern slopes of central Himalayas, north Bay of Bengal, and along the north of Western Ghats. As a result of these convergence zones over the Indo-Pakistan subcontinent, particularly along the Himalayan foothills, moisture is transported mainly from the Bay of Bengal to Pakistan. It is mentioned that the development of this moisture convergence zone is associated with the anticyclone located over the Tibetan plateau (Fig. 6a). Latif and Syed (2016) and Syed et al. (2010) also described the presence and significance of this convergence zone during the south Asian summer monsoon season. The results of EW-Rabi season (Fig. 7b) clearly show the presence of moisture flux convergence (negative anomaly; about − 2 kg m^{-2} s^{-1}) extending from north Pakistan along the Himalayas to the north Bay of Bengal. Another moisture convergence zone has been noticed over the north Arabian Sea. These negative anomalies are mainly responsible in advecting moisture from the Arabian Sea branch to the PPP, causing wet conditions over the region. Since eastward moving westerly troughs occasionally prevail during Rabi winter crop season, the moisture is therefore transported mainly from the west to the PPP. During annual time-scale (Fig. 7c), deeper moisture convergence progression has been observed from Bay of Bengal compared with the Arabian Sea. It can be concluded that the presence of moisture convergence anomalies over most of the Indo-Pakistan subcontinent, during seasonal and annual time-scales, is responsible in transporting moisture

Table 3 Details of wet and dry classes of precipitation with their respective grades based on percentile score, SPI, and RDI criteria

Years	Percentile			SPI			RDI		
	Kharif	Rabi	Annual	Kharif	Rabi	Annual	Kharif	Rabi	Annual
1981	ME	EW	LE	MW	N	MW	N	N	N
1982	N	EW	LE	MW	MW	MW	N	MW	N
1983	EW	MD	EW	EW	SW	SW	MW	N	MW
1984	LE	ED	N	N	N	N	N	N	N
1985	N	ME	N	N	N	N	N	N	N
1986	ED	N	MD	MD	N	N	N	N	N
1987	ED	MID	ED	N	N	N	MD	MD	MD
1988	LE	MD	MIE	N	N	N	N	N	N
1989	MD	N	MD	N	N	N	N	N	N
1990	LE	LE	EW	N	N	N	N	N	N
1991	MID	ME	N	N	N	N	N	N	N
1992	MIE	MID	ME	N	N	N	N	N	N
1993	MD	LD	LD	N	N	N	N	N	N
1994	EW	MIE	EW	MD	N	N	N	MW	N
1995	MIE	MIE	N	N	N	N	MW	N	N
1996	MID	MIE	N	N	N	N	N	N	N
1997	EW	LE	LE	SW	MW	MW	N	MW	MW
1998	N	MID	N	N	N	N	N	N	N
1999	LD	MD	LD	N	N	N	N	MD	N
2000	MD	ED	ED	N	N	N	MD	MD	MD
2001	ME	ED	MID	N	N	N	N	N	N
2002	MID	ME	LD	SD	MD	MD	N	MD	MD
2003	N	N	ME	N	N	N	N	N	N
2004	LD	LE	MD	N	N	N	N	N	N
2005	LD	LD	MID	MD	N	N	N	N	N
2006	MIE	EW	MIE	N	N	N	N	N	N
2007	ME	N	ME	N	N	N	MW	MW	MW
2008	N	N	MIE	MW	MW	MW	N	N	N
2009	ED	LD	ED	ED	MD	SD	MD	ED	SD
2010	N	–	MID	N	MD	MD	MD	N	MD

from Bay of Bengal and Arabia Sea, resulting in EW conditions over the Potwar region of Pakistan.

The VIMT and moisture flux convergence/divergence composite anomalies for ED cases on seasonal and annual time scales are shown in Fig. 7d–f. The positive moisture flux anomalies (divergence; > 1.5 kg m^{-2} s^{-1}) are present during the ED cases, which prevents the moisture transport form the Bay of Bengal and Arabian Sea to the PPP.

3.3.3 Precipitable water and vertical velocity anomalies

The composite anomalies of precipitable water for EW and ED Kharif, Rabi, and annual cases are presented in Fig. 8a–c and Fig. 8d–f, respectively. The precipitable water (or precipitable water vapor) is the depth of water vapor in a vertical column of atmosphere over unit cross-sectional area, if all the water vapor in that column were condensed as precipitation. It is a measure of atmospheric humidity which is an investigating tool of rainfall occurrence (Ferraro et al. 1998; Bhatia 2000). It is observed from Fig. 8a that a positive precipitable water anomaly (about 3 mm) with larger spatial extent is present over Pakistan and its adjoining areas during the EW-Kharif season. The presence of this positive anomaly can be considered as one of the main parameters of moisture availability and precipitation over the region. This positive anomaly is extending from Bay of Bengal to Pakistan, which is associated with the propagation of northward moving depressions from the Bay of Bengal during the Kharif (summer monsoon-dominated time) season. In Rabi season (Fig. 8b), the east-west elongated positive precipitable water vapor anomaly mainly extends from northwest Pakistan towards Tibetan Plateau, with center over Pakistan. The position and spatial

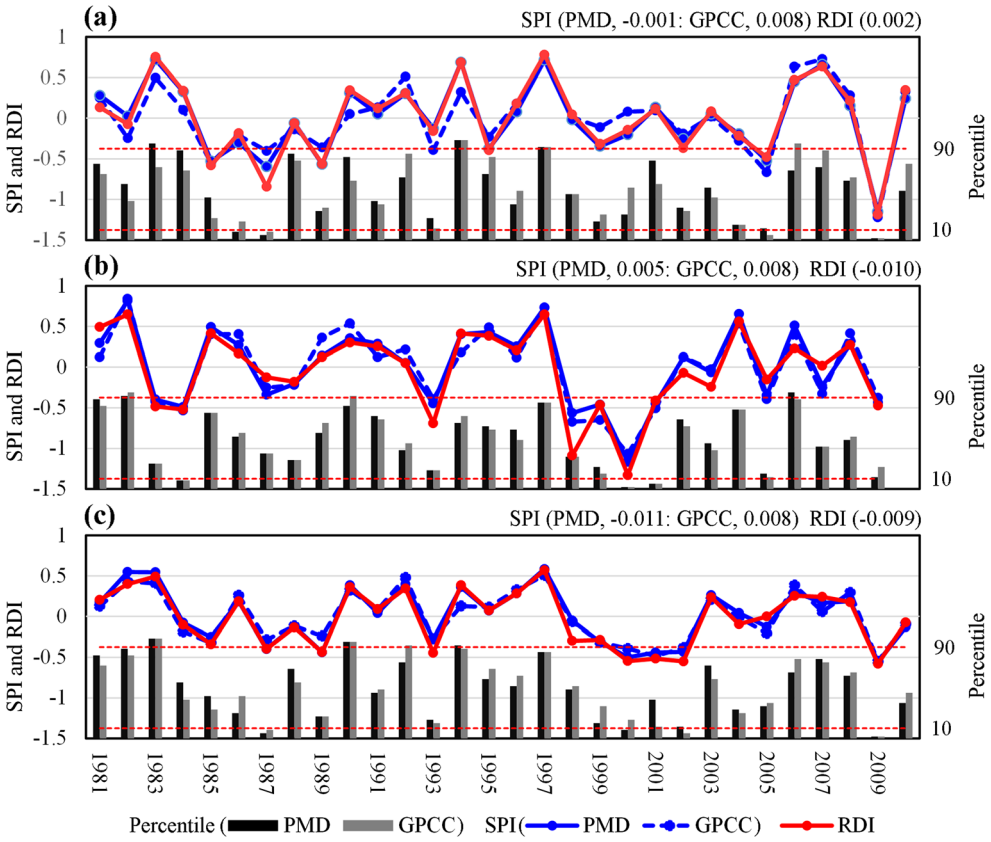

Fig. 4 (**a**): Time series comparison of SPI (blue) and RDI (red) drought indices for Kharif season for the period (1981–2010) using PMD (thick blue line) and GPCC (dotted blue line) datasets. Vertical bars on the secondary axis indicate percentile score using PMD (black) and GPCC (gray) datasets, whereas the horizontal dotted lines represent the 10th and 90th percentiles. The values in parenthesis show slope of trend line of SPI and RDI using Sen's slope estimator. The trend in time series is checked at 5% significance level using MK test. (**b**,**c**): Same as (**a**) except for Rabi and Annual cases, respectively

structure of this positive anomaly indicates its association with the eastward moving westerlies during the Rabi (affected by the western disturbances) season. Therefore, the water vapors transported from the Arabian Sea accumulate over the study

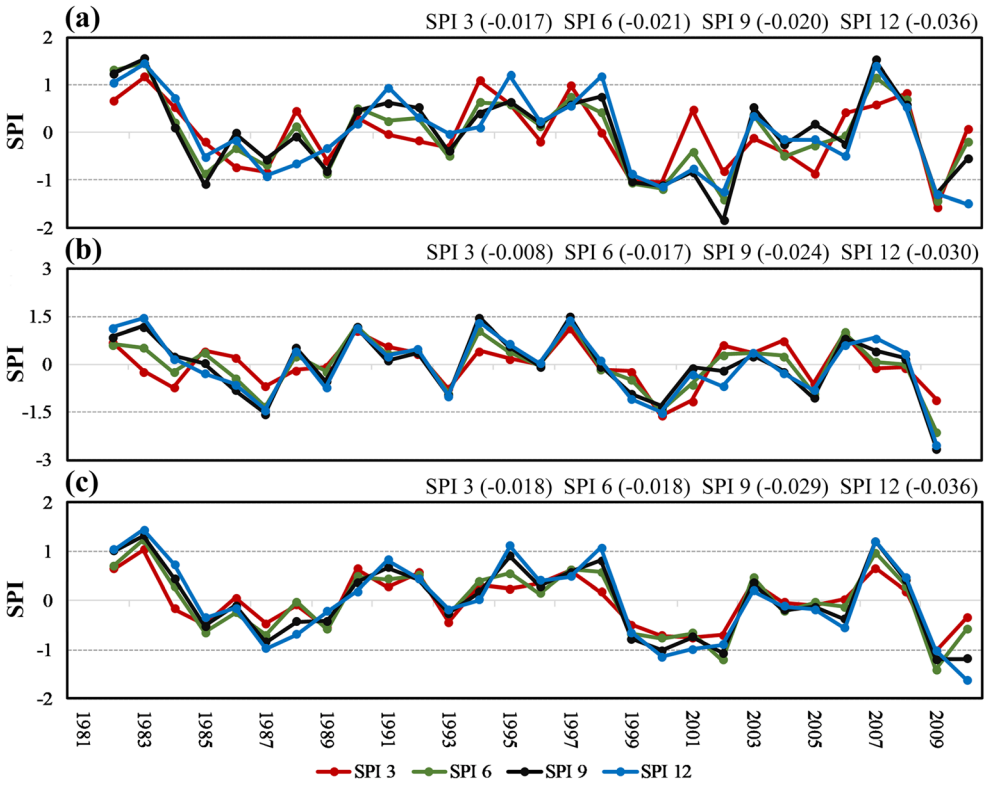

Fig. 5 (**a**): Time series comparison of SPI 3-, 6-, 9-, and 12-month aggregation time-scales for Kharif season for the period 1981 to 2010 using station datasets. The values in parenthesis show slope of trend line of SPI using Sen's slope estimator. The trend in time series is checked at 5% significance level using MK test. (**b**,**c**): Same as (**a**) except for Rabi and Annual cases, respectively

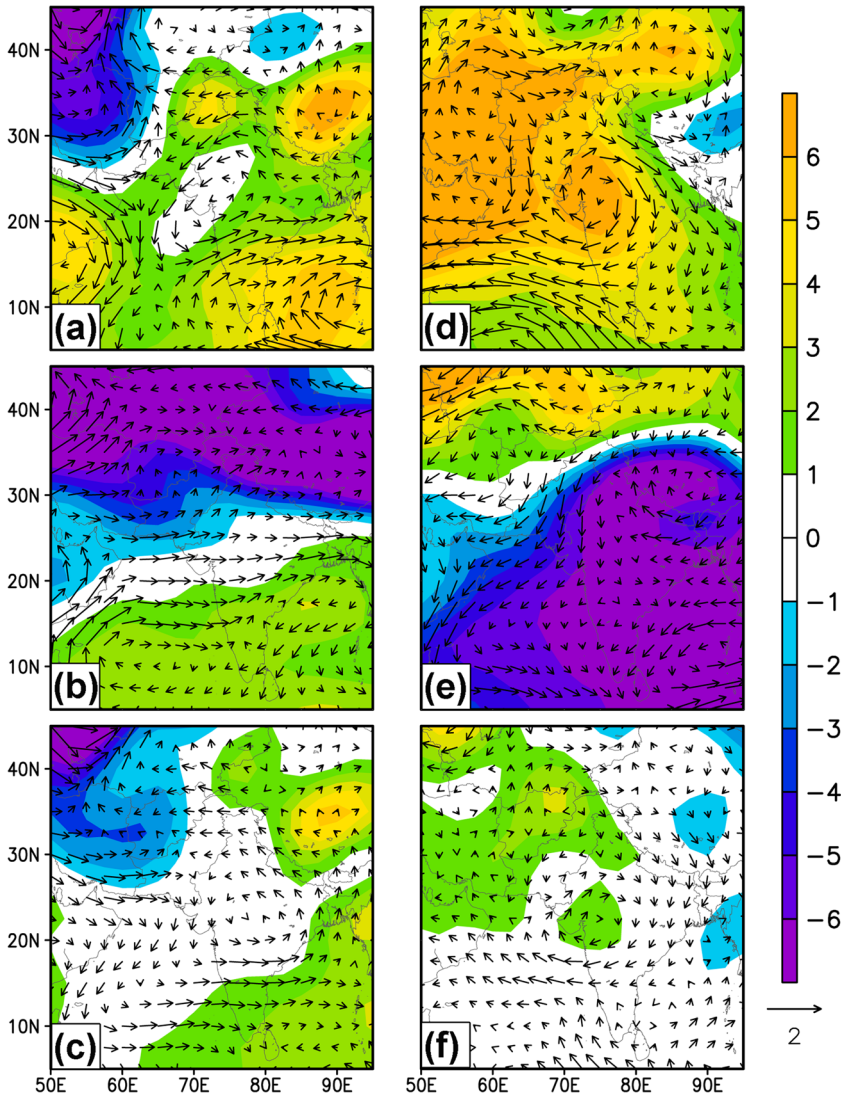

Fig. 6 Left panels (**a**–**c**): Geopotential height (shaded, units: meters) and wind (vector, units: m s^{-1}) composite anomalies at 850 hPa for EW cases during Kharif, Rabi, and annual time-scales. Right panels (**d**–**f**): same as left panels except for ED cases

region and cause precipitation during the season. The results of EW annual case show that almost the entire Indo-Pakistan subcontinent is dominated by the strong positive precipitable water anomaly, with more than 2 mm/month is observed over the eastern Indian Peninsula (partially over the eastern Ghats), Arabian Sea, and Pakistan (Fig. 8c). We may conclude that the higher precipitable water, associated with southwest summer monsoon (western disturbances), transported from the Bay of Bengal (Arabian Sea) directly contributes to Kharif (Rabi) precipitation amount. During ED Kharif, Rabi, and annual cases, the negative anomaly (− 2 mm) of precipitable water is dominated over most of the Indo-Pakistan subcontinent and its surrounding areas, contributing decisively in decreasing the precipitation amount over the region (Fig. 8d–f).

The composite anomalies of vertical velocity (omega) are presented at 500 hPa pressure level for EW (Fig. 9a–c) and ED (Fig. 9d–f) cases during Kharif, Rabi, and annual time-scales. A strong positive (negative) anomaly over northern (southern) half of the country is clearly visible in Fig. 9a. A positive anomaly is extended in northeast over Tibetan plateau and some parts of India and in the northwest over Afghanistan and Gulf region. On the other hand, a strong positive anomaly is still encompassing northern parts of the country extending towards south-western parts of the country (Fig. 9d), although its north-eastern and northwest extensions are no more there in this case. Important dominant factor is absence of strong negative anomaly in dry periods. It is now visible only in eastern part of southern half of the country with a weak intensity. In EW-Rabi case, a well-marked strong negative anomaly is clearly dominant over the country (Fig. 9b). On the other hand, a pronounced positive anomaly is distributed over the whole country during the ED-Rabi case (Fig. 9e). On annual time scale, almost same situation is prevailing as observed in EW and ED cases for both Kharif and Rabi seasons. Dominance of a strong negative anomaly over the country is a major feature of Fig. 9c, and it is absent in Fig. 9f, which

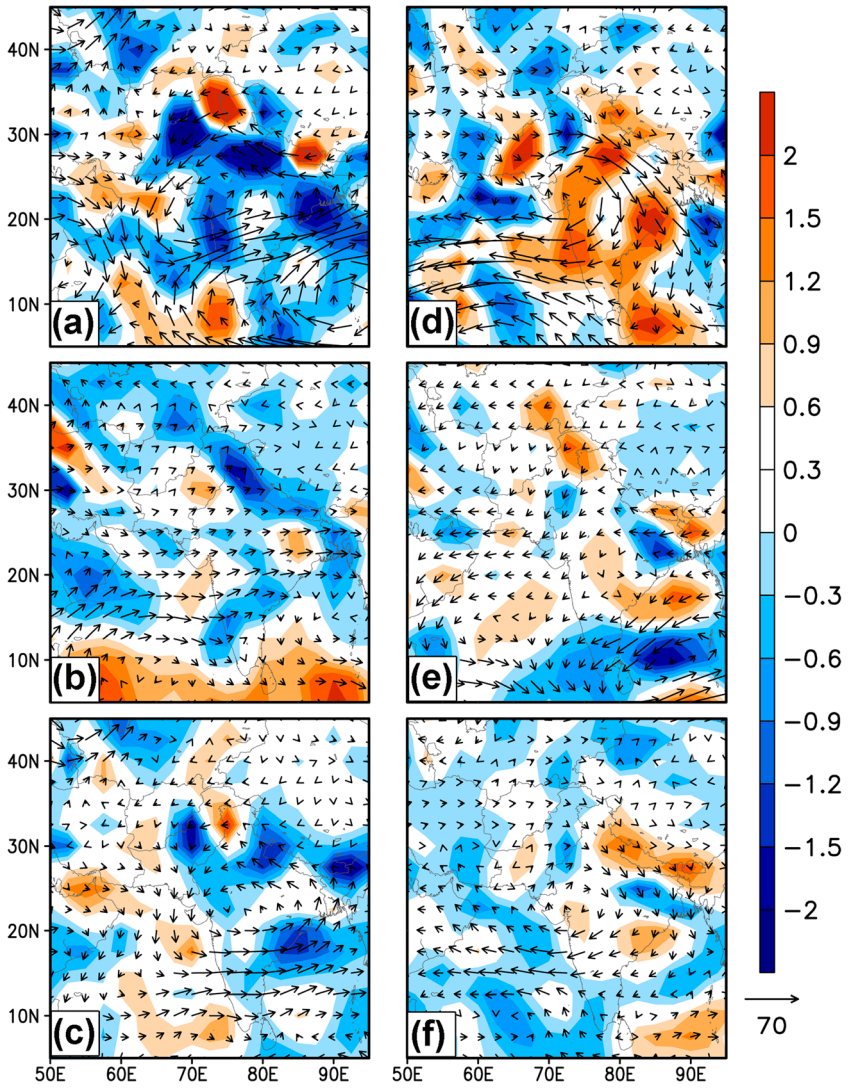

Fig. 7 Left panels (**a**–**c**): Composite anomaly of vertically integrated (surface to 300 hPa) moisture transport (vector, units: kg m^{-1} s^{-1}) and vertically integrated moisture flux convergence/divergence (shaded, units: kg m^{-2} s^{-1}) for EW cases during Kharif, Rabi, and annual time-scales, respectively. Right panels (**d**–**f**): same as left panels except for ED cases

shows a stronger positive anomaly over northern parts of the country. In dry periods, absence of channels of negative anomalies from Bay of Bengol and Arabian Sea in Kharif and Rabi seasons is highlighting the role of strong monsoon components and strong western disturbances, respectively, in dynamics of droughts over the region. In other words, a weak monsoon supports drought in Kharif and less precipitation in winter season supports drought in Rabi season. It is also noticeable that the role of Tibetan plateau during monsoon season is very crucial in determining precipitation variability over Pakistan (Wang et al. 2019).

Although some earlier studies explain the role of large-scale dynamical and thermo-dynamical characteristics of different circulation features over south Asia/Pakistan (see, for instance, Ahmed et al. 2019a, b; Latif et al. 2017; Syed et al. 2010), none of the studies explicitly investigated the role of dynamical mechanisms associated with drought and wetness conditions during two major cropping seasons (Kharif and Rabi) over the PPP. In this study, we have identified a clear role of Tibetan Plateau during Kharif (summer monsoon dominated) season, which plays an important role in transporting moisture from the Bay of Bengal and causes wet conditions over the region. Latif and Syed (2016) and Syed et al. (2010) have explained the role of the Tibetan Plateau; however, their results show that although weather-producing low pressure systems come from the Bay of Bengal, the moisture is mainly transported from the Arabian Sea during summer (July–September) and rainy seasons. Our results in relation to the identification of positive height anomaly (anti-cyclone) over Tibetan Plateau and associated moisture transport from the Bay of Bengal during Kharif season is a new contribution to the existing literature. Since, this study explains a physical linkage between large-scale dynamics and drought/wetness conditions, the same association could be studied in the future using regional or global climate models to see why the trends of drought severity are increasing in the future. This will be helpful in understanding the large-scale dynamics of future projected droughts.

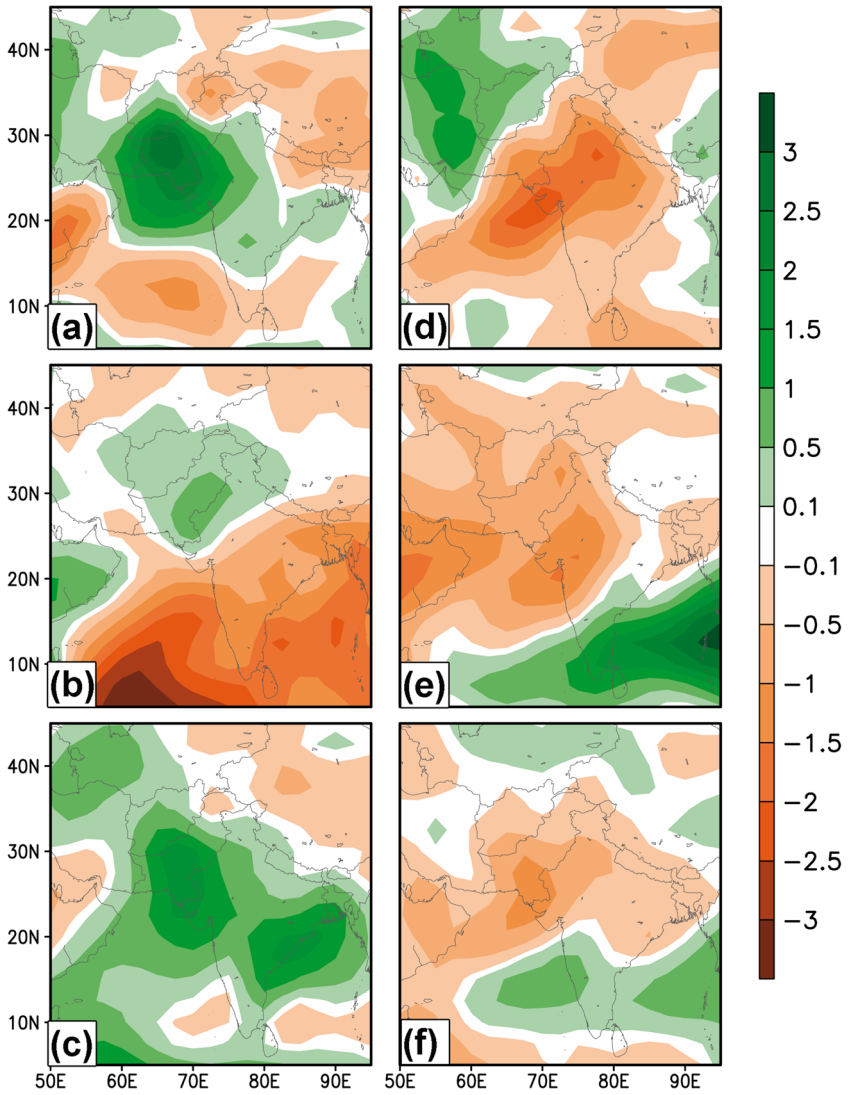

Fig. 8 Left panels (**a**–**c**): Precipitable water composite anomalies (units: mm) for EW cases during Kharif, Rabi, and annual time-scales, respectively. Right panels (**d**–**f**): same as left panels except for ED cases

3.4 Analysis of future drought characteristics

3.4.1 Model selection and evaluation

In this section, future drought conditions are studied by using CORDEX south Asia RCM (RegCM4.4 and RCA4) simulations. We first selected the best performing model datasets using RCM outputs driven by different GCMs as LBCs (Table 1). The selection of model is based on a statistical comparison of precipitation between the model outputs for the historical run (1981–2005) and PMD station datasets (observations) over the PPP (Fig. 10). It can be clearly seen from the figure that the RegCM4.4 model, driven by CCMA-CanESM2 GCM as boundary conditions, best correlates with the observations. This model has a relatively high correlation and smaller RMSE, and the standard deviation (STDV) is closer to the observations. Although RCM4.4 (run with CNRM-CM5 GCM as LBCs) has mean closer to the station data, the RMSE and STDV do not approximate well with observations. In addition, the mean of RegCM4.4 (GFDL-ESM2M) is noted within the range of half of STDV, but the spread of maximum and minimum values is very large. It is also noted that RCA4, which run with CCMA-CanESM2, IPSL-CM5A-MR, and CSIRO-MK3.6.0 LBCs, do not perform well with the observations over the Potwar region of Pakistan.

The performance of selected RCM model, i.e., RegCM4.4 with CCMA-CanESM2 GCM as LBCs, with so-called perfect boundary conditions (ERA-Interim) and GPCC precipitation is further evaluated for the present (1981–2005) climate over the PPP (Fig. 11). Figure 11 (top row) shows the spatial pattern of observed (GPCC) precipitation climatology for Kharif, Rabi, and annual time-scales, respectively, over the region. The Core Monsoon Region of Pakistan (CMRP, Latif et al. 2017) receives the highest amount of precipitation during the Kharif season (Fig. 11a), as the region is influenced by the penetration of weather-producing low pressure systems from the Bay of Bengal (Latif and Syed 2016; Faisal and Sadiq

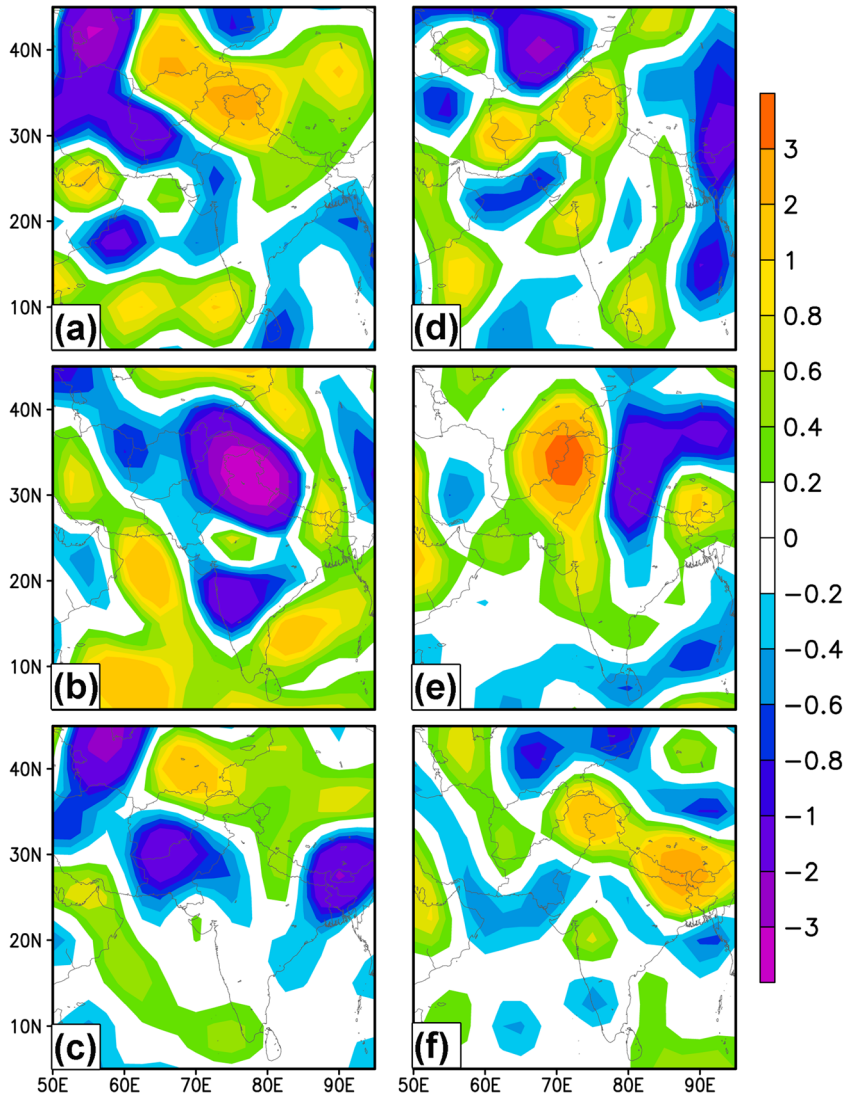

Fig. 9 Left panels (**a**-**c**): Omega (vertical velocity) composite anomalies (units: $\times 10^{-2}$ Pa S^{-1}) at 500 hPa for EW cases during Kharif, Rabi, and annual time-scales, respectively. Right panels (**d**–**f**): same as left panels except for ED cases

2012). In the Rabi season, the CMRP and its adjoining eastern regions again received the highest amount of precipitation, caused by the eastward moving western disturbances (Fig. 11d). The annual time-scale shows the contribution of precipitation of both Kharif and Rabi seasons (Fig. 11g). It is observed from Fig. 11 (middle row) that the spatial patterns of seasonal and annual mean precipitation in RegCM4.4 (driven by Era-Interim LBCs) is consistent with the observations (GPCC). However, the model simulates slightly more precipitation (particularly in Rabi season) over the north, north-eastern parts of Pakistan, and along the foothills of the western Himalayas. The RegCM4.4 simulations with global model CCCMA-CanESM2 as LBCs are quite consistent with the model's Era-Interim run (Fig. 11, bottom row), but a wet bias is noted along the coastal belt of Pakistan during the Kharif season. This indicates that the selected model RegCM4.4 (CCCMA-CanESM2) shows a reasonable skill in capturing the spatial pattern of seasonal and annual mean precipitation, but with slight overestimates (wet bias) over the region where summer and winter precipitation-producing weather systems prevail.

3.4.2 Changes in future drought with RegCM4.4 projections

In order to analyze future drought frequency, severity, and trends over the PPP on seasonal (Kharif and Rabi) and annual basis using SPI and RDI drought indices, RegCM4.4 model simulation with CCCMA-CanESM2M GCM LBCs for two RCP scenarios, i.e., RCP4.5 and RCP8.5, are used. The analysis was performed for two time periods, i.e., reference period (1981–2005) and future projections (2006–2100).

The SPI and RDI results using RegCM4.4 (CCCMA-CanESM2M) simulations are presented in Fig. 12 (top panel) and (bottom panel), respectively. SPI results for the historical period show a negative slope of trend line for Kharif, Rabi, and annual time scales (Fig. 12a–c, top panel), which are

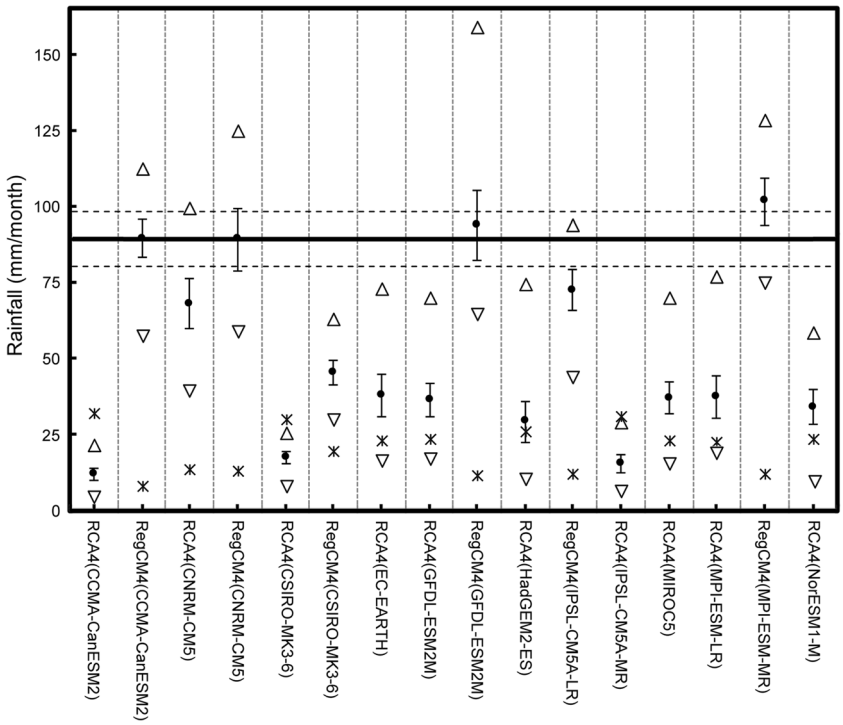

Fig. 10 Statistical comparison of precipitation (units: mm/month) between RCM simulations and station datasets for the baseline period 1981–2005. Black horizontal thick line shows mean precipitation using station data, whereas the dashed horizontal lines show mean plus/minus half standard deviation (STDV). Black circles with error bar show mean and mean plus/minus half STDV of RCMs driven by different GCMs as LBCs. Up and down triangles show maximum and minimum values, whereas asterisk represents the RMSE

consistent with the baseline observation (Fig. 4). The future SPI monthly time series show a positive slope of trend line for Kharif, Rabi, and annual time-scales under both RCP4.5 and RCP8.5 scenarios; however, Rabi witnesses a negative trend under RCP4.5 scenario. The results of the slope (negative) of trend line of RDI for the historical period (Fig. 12a–c, bottom panel) are again consistent with the baseline observations. The future RDI time series shows positive trend for Kharif and

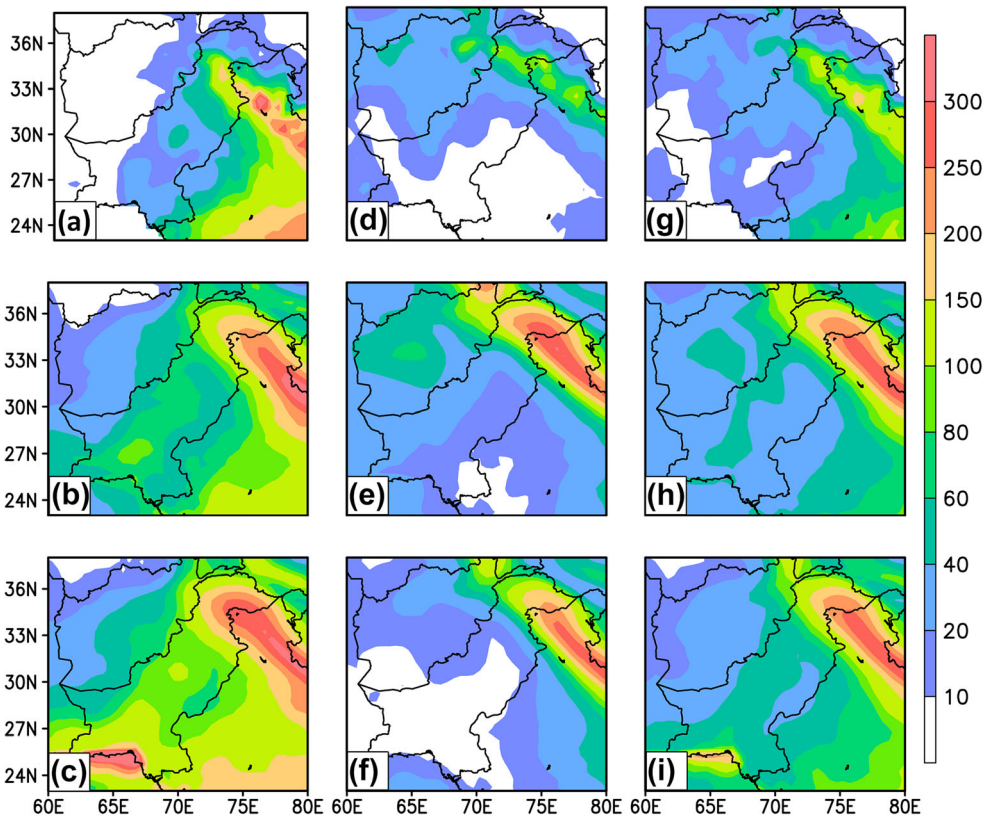

Fig. 11 Left panels (**a**): Precipitation climatology (units: mm/month) for Kharif season using GPCC data for the period from 1981 to 2005. (**b**,**c**): Same as (**a**) except for RegCM4-4 with Era-Interim and CCCMA-CanESM2 as LBCs, respectively. Middle and right panels (**d**–**f**) and (**g**–**i**): same as left panels except for Rabi and annual basis, respectively

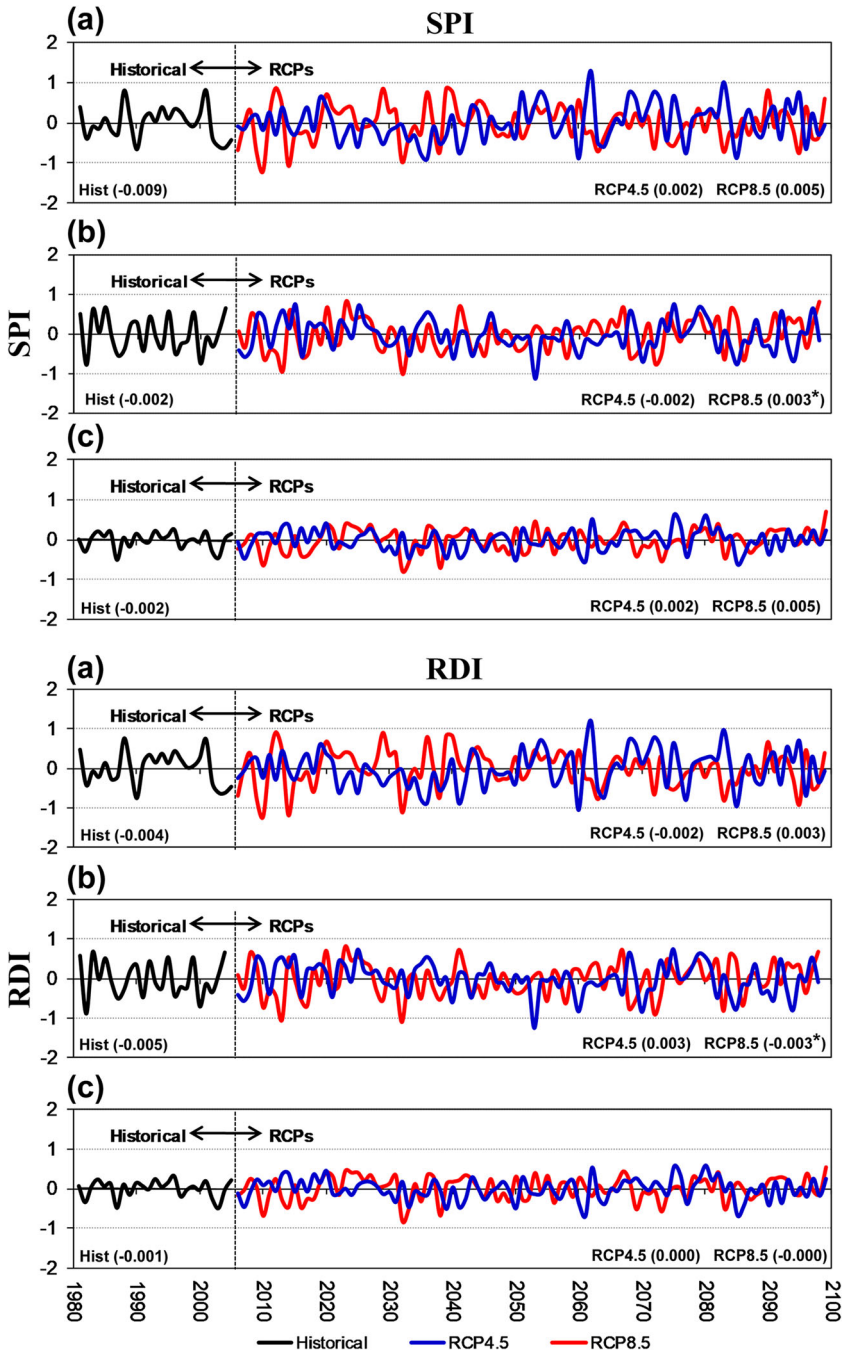

Fig. 12 Top panel (**a**–**c**): Time series comparison of SPI for Kharif, Rabi, and annual time-scales, respectively, based on RegCm4.4 (CCCMA-CanESM2M) outputs, under RCP4.5 and RCP8.5 scenarios. Bottom panel (**a**–**c**): Same as top panel except for RDI. The values in parenthesis show slope of trend line of SPI and RDI. The trend in time series is checked at 5% significance level and is marked with asterisk

Rabi seasons under both RCP scenarios, whereas the annual showed almost no trend in the time series of the future.

The results of SPI on 3-, 6-, 9-, and 12-month aggregation time-scales are presented in Fig. 13. It is observed from Fig. 13 that negative slope of trend line for all time-scales (SPI 3, 6, 9, and 12) for both Rabi and annual bases is well captured by the ReghCM4.4. However, results of SPI 3, 6, and 12 for Kharif season are not consistent with the baseline observation. The future RCPs show almost positive (towards wetness) slope of trend line for both seasonally and annually. The slope of trend line is statistically significant (at 5% significance level) for longer time-scale for Kharif season (SPI 12) as well as annually (SPI 9 and SPI 12 under RCP 4.5 scenario) (Fig. 13). The drought years are further calculated on seasonal and annual basis for all time-scales (Table 4). SPI 3 and SPI 6 analyses show maximum number of moderate level droughts during Kharif season under both RCP scenarios. In Rabi season, severe (3) and extreme (2) level droughts are identified under RCP4.5 and RCP8.5 scenarios, respectively. Based on SPI 9, it is noted that the maximum number

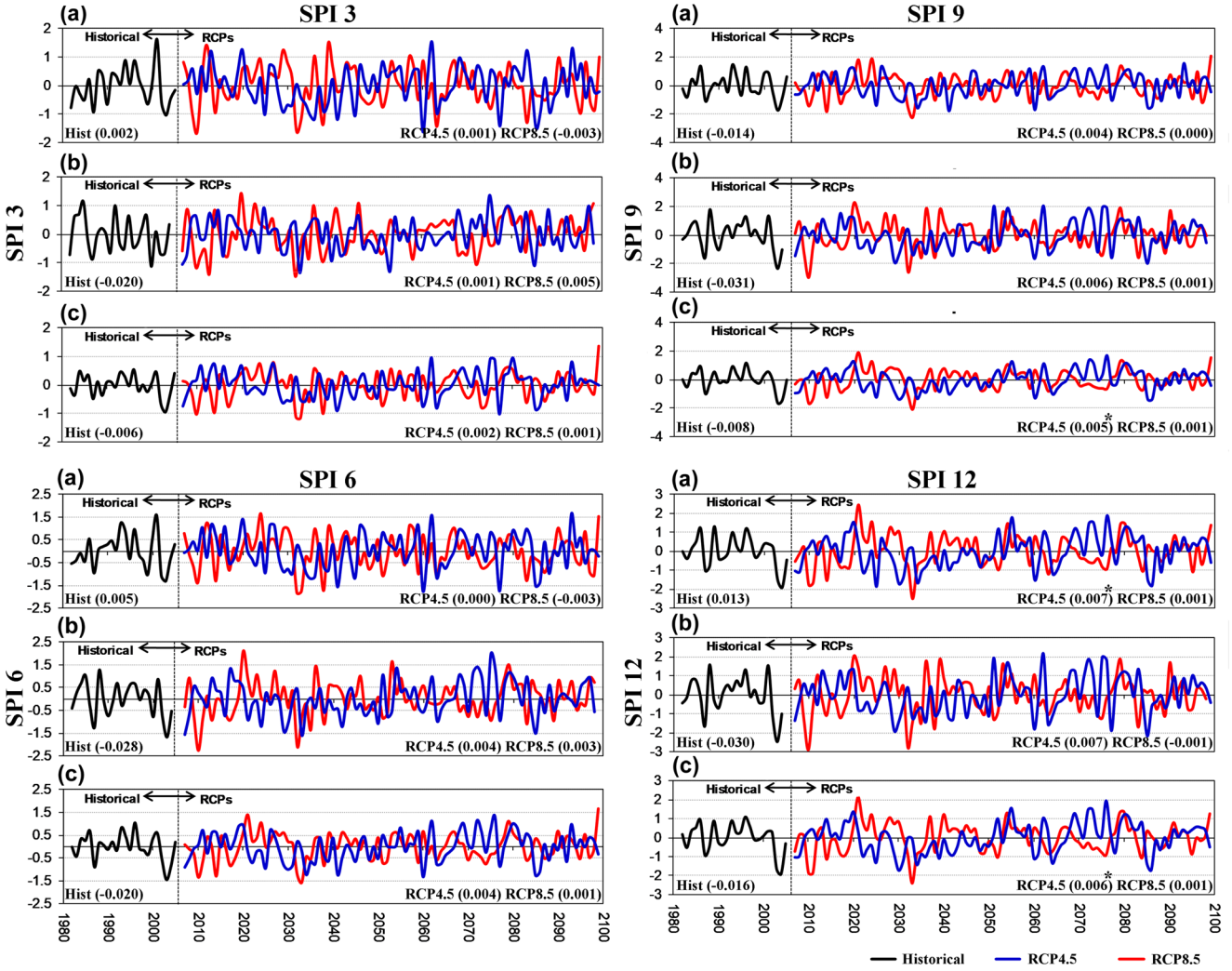

Fig. 13 Time series comparison of SPI 3-, 6-, 9-, and 12-month aggregation time-scales for Kharif (**a**), Rabi (**b**), and annual (**c**) bases, using RegCM4.4 driven by CCCMA-CanESM2M LBCs under RCP4.5 and RCP8.5 scenarios. The values in parenthesis show slope of trend line of SPI. The trend in time series is checked at 5% significance level and is marked with asterisk

of moderate level drought (12 out of 16 under RCP 4.5 and 6 out of 11 under RCP8.5) is observed during Rabi season, compared with the Kharif season. The results of SPI 12 show similar behavior during the Rabi season.

It is clear from Table 4 that the Kharif season is more vulnerable to short time-scale, whereas the Rabi is more vulnerable to long time-scale. It is interesting to note that the total number of droughts observed for annual cases (under both RCP scenarios) is less than that of seasonal basis, which clearly provides evidence that the Potwar region is strongly affected by the seasonal droughts as compared with the annual droughts. Moreover, the total number of drought and its intensity are less for shorter time-scales (SPI 3 and SPI 6) and more for longer time-scales (SPI 9 and SPI 12). Adnan et al. (2015) conducted a similar study over the Sindh province of Pakistan and found that the frequency of intense droughts may not be observed on shorter time-scales (e.g., SPI 3 or less). Our results also suggest that the drought events under RCP8.5 are less compared with RCP 8.5 on both seasonal and annual bases. In general, no significant trends of droughts are observed in the future under both RCP scenarios for the two cropping seasons. However, a positive slope of trend line of both SPI and RDI indicates an increasing trend towards wetness over the region, which may be attributed to the increasing trends of rainfall and moisture transport from the Arabian Sea (Latif et al. 2018).

4 Summary and conclusions

Drought is one of the most frequently occurring natural hazards, which has serious impacts on the agricultural sector. There have been many studies conducted in the past, but drought assessment and its related large-scale atmospheric

Table 4 Details of extreme, severe, and moderate classes of drought based on SPI 3-, 6-, 9-, and 12-month aggregation time-scales for RegCM4.4, driven by CCMA-CanESM2 LBCs, under RCP 4.5 and RCP 8.5 scenario

Time scale	Season/ annual	Drought classes							
		RCP4.5				RCP8.5			
		Extreme	Severe	Moderate	Total	Extreme	Severe	Moderate	Total
SPI 3	Kharif		1	7	8		2	5	7
	Rabi			4	4			4	4
	Annual			1	1			4	4
SPI 6	Kharif		4	7	11		3	6	9
	Rabi		3	5	8	2		3	5
	Annual			5	5		1	3	4
SPI 9	Kharif		4	7	11	1	2	6	9
	Rabi		4	12	16	2	3	6	11
	Annual			9	9	1	1	3	5
SPI 12	Kharif		5	9	14	1	3	3	7
	Rabi	1	4	11	16	2	2	11	15
	Annual		2	9	11	1	2	3	6

dynamics as well as the future projections using RCMs for two major cropping seasons, i.e., Kharif and Rabi, over the Potwar Plateau of Pakistan (PPP), have not yet been studied over Pakistan. The agricultural activities of this region are highly dependent on rain water.

In this study, past and future droughts over the PPP are investigated along with related large-scale dynamics on seasonal and annual time-scales. The analyses are performed using station, observed, reanalysis, and RCM datasets, for the past (1981–2010) and future (2011–2100) time periods. For the identification of EW and ED cases of precipitation, the percentile rank approach and drought indices (SPI and RDI) are used. Future projections of droughts are investigated using RegCM4.4 and RCA4 model outputs under RCP4.5 and RCP8.5 scenarios. Our results show that, among six observational/reanalysis datasets, GPCC (for precipitation) and APHRODITE (for temperature) approximate well with the station data during both Kharif and Rabi seasons. It is also observed that the Era-interim reanalysis does not perform well for both precipitation and temperature cases.

By employing percentile score, SPI, and RDI criteria, we found that SPI-based cases of precipitation deficit and surplus are almost equal in Kharif and Rabi seasons; however, surplus cases on annual time-scale are slightly higher than deficit. The RDI results are consistent with the SPI. The percentile, SPI, and RDI results show the years 1986, 1987, 2002, and 2009 as driest, whereas the wet cases are noted during 1987, 1994, and 1997. The SPI and RDI results correlate well with percentile score method. SPI shows a positive slope of trend line for both seasonal and annual bases using GPCC but a negative trend line slope (positive) in Kharif (Rabi) season for the station data. A positive slope of RDI is observed for Kharif and negative for Rabi and annual cases. SPI is further calculated at 3-, 6-, 9-, and 12-month aggregation time-scales. The results show a negative slope on both seasonal and annual time-scales, indicating decreasing trends (towards drought). Due to the high rainfall variability over the PPP and its geographical location (receives highest amount of rainfall both in summer and winter seasons), drought period usually remains for a shorter time period and less intense as compared with other parts of the country.

The composites of geopotential height and wind anomalies show that, during EW-Kharif (EW-Rabi) season, Tibetan anticyclone (westerly flow) plays a crucial role in moisture incursion from the Bay of Bengal (Arabian Sea) for wet conditions over the study region. The results are the same for ED cases, but with a reverse sign of anomalies. The composite anomalies of integrated moisture transport and moisture flux convergence/divergence show that the presence of moisture convergence anomalies over most of the Indo-Pakistan subcontinent during seasonal and annual time-scales is responsible for transporting moisture from Bay of Bengal and Arabia Sea, resulting in EW conditions over the study region. Our results in relation to the identification of positive height anomaly (anti-cyclone) over the Tibetan Plateau and associated moisture transport from the Bay of Bengal during Kharif season are a new contribution to the existing literature. The precipitable water composite anomalies show higher precipitable water amount, associated with summer monsoon (western disturbances), transported from the Bay of Bengal (Arabian Sea), which contributes directly to Kharif (Rabi) rainfall amount over the region. The vertical velocity results indicate the important role of negative (positive) anomalies during EW (ED) cases.

Future drought conditions are further investigated using RegCM4.4 and RCA4 outputs, driven by different GCMs

as LBCs, from CORDEX south Asia domain. The RegCM4.4 model run with CCMA-CanESM2 LBCs is found to approximate well with the observations. The performance of selected RegCM4.4 is further evaluated with ERA-Interim LBCs and GPCC precipitation and found that the RegCM4.4 model shows a reasonable skill in capturing spatial pattern of seasonal and annual mean precipitation. Based on the selected RegCM4.4 model outputs, the SPI and RDI results for the historical period show negative (towards drought) slope of trend line, which are consistent with the baseline observations. The future SPI and RDI monthly time series show a positive (towards wetness) trend for Kharif, Rabi, and annual time-scales under both RCP scenarios. The negative trends for SPI 3-, 6-, 9-, and 12-month time-scales are well captured by the ReghCM4.4 model for both Kharif and annual cases; however, the results of Kharif season are not consistent with the baseline observations. The projected changes in droughts using SPI and RDI under both RCPs show weak positive trend for both seasonally and annually, which could be linked to an increasing trend of rainfall and moisture transport from the Arabian Sea. Given this study explains a physical linkage between large-scale dynamics and drought/wetness conditions, the same association could be studied in the future using regional or global climate models to see why the trends of drought severity are increasing in the future. This will be helpful in understanding the large-scale dynamics of future projected droughts.

This study will provide assistance for the long-term forecast of drought and to develop an early warning system of drought occurrence. It will be useful in developing contingency strategies for the rain water-dependent region that will ultimately be used for guiding water resource management practices, increasing agricultural yield, and improving ecological protection and socio-economic growth. The study will also be helpful in enhancing the competence of humanitarian response in order to handle extreme weather conditions.

Acknowledgments The authors thank the CORDEX framework, initiated and funded by the World Climate Research Program (WCRP), for providing the regional climate models (RCA4 and RegCM4.4) datasets for South Asia region available at Earth System Grid Federation (ESGF) data portal and hosted at the Swedish Meteorological and Hydrological Institute (SMHI) and Indian Institute of Tropical Meteorology (IITM), respectively. The authors are also thankful to the European Centre for Medium-Range Weather Forecast (ECMWF) and NCEP (National Center for Environmental prediction)/NCAR (National Center for Atmospheric Research) for providing access to the reanalysis data products. We are grateful to the developers of GPCC, CRU, UDEL, and PREC/L for providing gridded observed precipitation and temperature datasets. We also acknowledge Climate Data Processing Centre (CDPC) Karachi and Pakistan Meteorological Department (PMD) for the monthly station datasets. This research was funded by the Pakistan Science Foundation (Grant Number: PSF/NSFC-Earth/C-COMSATS-lsb (07)) and Higher Education Commission of Pakistan (Grant Number: 8035/Balochistan/NRPU/R&D/HEC/2017).

References

Adnan S, Haider S (2012) Classification and assessment of aridity over Pakistan provinces (1960-2009). International Journal of Environment 3(4):24–35

Adnan S, Khan AH (2009) Effective rainfall for irrigated agriculture plains of Pakistan. Pakistan Journal of Meteorology 6(11):61–72

Adnan S, Mahmood R, Khan AH (2009) Water balance conditions in rainfed areas of Potohar and Balochistan plateau during 1931-08. World Appl Sci J 7(2):162–169

Adnan S, Ullah K, Gao S (2015) Characterization of drought and its assessment over Sindh, Pakistan during 1951–2010. Journal of Meteorological Research 29(5):837–857

Adnan S, Ullah K, Shouting G (2016) Investigations into precipitation and drought climatologies in South Central Asia with special focus on Pakistan over the period 1951–2010. J Clim 29(16):6019–6035

Adnan S, Ullah K, Khan AH, GAO S (2017) Meteorological impacts on evapotranspiration in different agro-climatic zones of Pakistan. Journal of Arid Land 9(6):938–952

Adnan S, Ullah K, Shuanglin L, Gao S, Khan AH, Mahmood R (2018) Comparison of various drought indices to monitor drought status in Pakistan. Clim Dyn 51(5–6):1885–1899

Ahmad B, Hussain A (2017) Evaluation of past and projected climate change in Pakistan region based on GCM20 and RegCM4. 3 outputs. Pakistan Journal of Meteorology 13(26):63–86

Ahmed F, Adnan S, Latif M (2019a) Impacts of winter jet stream and associated mechanisms over winter precipitation variability modes over Pakistan. Meteorology and Atmospheric Physics:1–14. https://doi.org/10.1007/s00703-019-00683-8

Ahmed K, Shahid S, Wang X, Nawaz N, Najeebullah K (2019b) Evaluation of gridded precipitation datasets over arid regions of Pakistan. Water 11(2):210

Ali S, Khattak MS, Khan D, Sharif M, Khan H, Ullah A, Malik A (2016) Predicting future temperature and precipitation over Pakistan in the 21st century. Journal of Engineering and Applied Sciences 35(2): 61–76

Anjum S, Wang L, Salhab J, Khan I, Saleem MF (2010) An assessment of drought extent and impact in agriculture sector in Pakistan. Journal of Food, Agriculture and Environment 8(3/4 part 2):1359–1363

Ashraf M (2004) Impact evaluation of water resources development in the command area of small dams. Pakistan Council of Research in Water Resources (PCRWR), research report 5-2004

Bhatia RC (2000) Use of SSM/I derived products for diagnostic studies of heavy rainfall events over coastal area of India. TROPMET 2000: 281–285

Cakir R (2004) Effect of water stress at different development stages on vegetative and reproductive growth of corn. Field Crop Res 89(1):1–16

Cheema SB, Hanif M (2013) Seasonal precipitation variation over Punjab province. Pakistan Journal of Meteorology 10(19):61–82

Chen M, Xie P, Janowiak JE, Arkin PA (2002) Global land precipitation: a 50-yr monthly analysis based on gauge observations. J Hydrometeorol 3(3):249–266

Dee DP, Uppala SM, Simmons AJ, Berrisford P, Poli P, Kobayashi S, Andrae U, Balmaseda MA, Balsamo G, Bauer P, Bechtold P, Beljaars AC, van de Berg L, Bidlot J, Bormann N, Delsol C, Dragani R, Fuentes M, Geer AJ, Haimberger L, Healy SB, Hersbach H, Hólm EV, Isaksen L, Kållberg P, Köhler M, Matricardi M, McNally AP, Monge-Sanz BM, Morcrette J, Park B, Peubey C, de Rosnay P, Tavolato C, Thépaut J, Vitart F (2011) The ERA-interim reanalysis: configuration and performance of the data assimilation system. Quarterly Journal of Royal Meteorological Society 137(656):553–597

Faisal N, Sadiq N (2012) Monsoon onset over selected eastern boundary cities of Pakistan. Nucleus 49(3):239–245

Ferraro RR, Kusselson SJ, Colton M (1998) An introduction to passive microwave remote sensing and its applications to meteorological analysis and forecasting. Natl Wea Dig 22:11–23
Gibbs J, Maher J (1967) Rainfall deciles as drought indicators. Bureau of Meteorology Bulletin No. 48, Commonwealth of Australia, Melbourne
Gilbert RO (1987) Statistical methods for environmental pollution monitoring. Van Nostrand Reinhold, NewYork
Giorgi F, Jones C, Asrar GR (2009) Addressing climate information needs at the regional level: the CORDEX framework. World Meteorological Organization (WMO) Bulletin 58(3):175–183
Giorgi F, Coppola E, Solmon F, Mariotti L, Sylla MB, Bi X, Turuncoglu UU (2012) RegCM4: model description and preliminary tests over multiple CORDEX domains. Clim Res 52:7–29
Gonzalez-Hidalgo JC, Lopez-Bustins JA, Štepánek P, Martin-Vide J, de Luis M (2009) Monthly precipitation trends on the Mediterranean fringe of the Iberian Peninsula during the second-half of the twentieth century (1951–2000). Int J Climatol 29(10):1415–1429
Haider S, Adnan S (2014) Classification and assessment of aridity over Pakistan provinces (1960-2009). International Journal of Environment 3(4):24–35
Hao Z, Aghakouchak A (2014) A nonparametric multivariate multi-index drought monitoring framework. J Hydrometeorol 15:89–101
Hao Z, Hao F, Singh VP, Xia Y, Ouyang W, Shen X (2016) A theoretical drought classification method for the multivariate drought index based on distribution properties of standardized drought indices. Adv Water Resour 92:240–247
Haroon MA, Zhang J, Yao F (2016) Drought monitoring and performance evaluation of MODIS-based drought severity index (DSI) over Pakistan. Nat Hazards 84(2):1349–1366
Harris IPDJ, Jones PD, Osborn TJ, Lister DH (2014) Updated high-resolution grids of monthly climatic observations—the CRU TS3. 10 dataset. Int J Climatol 34(3):623–642
Hisdal H, Stahl K, Tallaksen LM, Demuth S (2001) Have stream flow droughts in Europe become more severe or frequent? Int J Climatol 21(3):317–333
Hussain MS, Lee S (2009) A classification of rainfall regions in Pakistan. Journal of Korean Geographical Society 44(5):605–623
IUCN (2009) Proceeding, workshop on "Stabilizing climate change in the Himalayas" held on 04 August 2009, Nepal
Kalnay E, Kanamitsu M, Kistler R, Collins W, Deaven D, Gandin L, Iredell M, Saha S, White G, Woollen J, Zhu Y, Chelliah M, Ebisuzaki W, Higgins W, Ropelewski C, Wang J, Leetmaa A, Reynolds R, Jenne R, Joseph D (1996) The NCEP/NCAR 40-year reanalysis project. Bull Am Meteorol Soc 77(3):437–471
Kant SKS, Meshram S, Sahu KC (2014) Analysis of rainfall data for drought investigation at Agra UP. Recent Research in Science and Technology, 6(1). https://updatepublishing.com/journal/index.php/rrst/article/view/1166. Accessed 12 Aug 2019
Kao SC, Govindaraju RS (2010) A copula-based joint deficit index for droughts. J Hydrol 380(1–2):121–134
Kendall MG (1975) Rank correlation methods. Charles Griffin, London
Kreft S, Eckstein D, Junghans L, Kerestan C, Hagen U (2013) Global climate risk index 2014. Global climate risk index 2014. Who suffers most from extreme weather events, p. 1Á31
Latif M, Syed FS (2016) Determination of summer monsoon onset and its related large-scale circulation characteristics over Pakistan. Theor Appl Climatol 125(3–4):509–520
Latif M, Syed FS, Hannachi A (2017) Rainfall trends in the South Asian summer monsoon and its related large-scale dynamics with focus over Pakistan. Clim Dyn 48(11–12):3565–3581
Latif M, Hannachi A, Syed FS (2018) Analysis of rainfall trends over Indo-Pakistan summer monsoon and related dynamics based on CMIP5 climate model simulations. Int J Climatol 38:e577–e595
Le Houérou HN (1996) Climate change, drought and desertification. Journal of Arid Environments 34(2):133–185
Ma W, Huang W, Yang Z, Wang B, Lin D, He X (2018) Dynamic and thermodynamic factors associated with different precipitation regimes over South China during pre-monsoon season. Atmosphere 9(6):219
Mann HB (1945) Nonparametric tests against trend. Econometrica 13(3): 245–259
McKee TB, Doesken NJ, Kliest J (1993) The relationship of drought frequency and duration to time scales. In Proceedings of the 8th Conference on Applied Climatology, 17–22 January, Anaheim, CA. American Meteorological Society, Boston, pp 179–184
Mendicino G, Senatore A, Versace P (2008) A groundwater resource index (GRI) for drought monitoring and forecasting in a Mediterranean climate. J Hydrol 357(3–4):282–302
Moss T, Babiker M, Brinkman S, Calvo E, Carter T, Edmonds J, Elgizouli I, Emori S, Erda L, Hibbard K, Jones R, Kainuma M, Kelleher J, Lamarque JF, Manning M, Matthews B, Meehl G, Meyer L, Mitchell J, Nakic'enovic' N, O'Neill B, Pichs T, Riahi K, Rose S, Runci P, Stouffer R, van Vuuren D, Weyant J, Wilbanks T, van Ypersele JP, Zurek M (2008) Towards new scenarios for analysis of emissions, climate change, impacts, and response strategies. Intergovernmental Panel on Climate Change, Geneva, p 132
Narasimhan B, Srinivasan R (2005) Development and evaluation of Soil Moisture Deficit Index (SMDI) and Evapotranspiration Deficit Index (ETDI) for agricultural drought monitoring. Agric For Meteorol 133(1–4):69–88
Palmer WC (1965) Meteorological drought. Disasters 30:1–58
Palmer WC (1968) Keeping track of crop moisture conditions, nationwide: the new crop moisture index. Weather Wise 21(4):156–161
Pasha M, Ali A, Waheed A (2015) Sindh drought 2014—Pakistan: was it a natural or a man-made disaster? American Journal of Social Science Research 1(1):16–20
Pashiardis S, Michaelides S (2008) Implementation of the standardized precipitation index (SPI) and the reconnaissance drought index (RDI) for regional drought assessment: a case study for Cyprus. European Water 23(24):57–65
Pietzsch S, Bissolli P (2011) A modified drought index for WMO RA VI. Adv Sci Res 6(1):275–279
Raible CC, Bärenbold O, Gomez-Navarro JJ (2017) Drought indices revisited—improving and testing of drought indices in a simulation of the last two millennia for Europe. Tellus A: Dynamic Meteorology and Oceanography 69(1):1287492
Rashid K, Rasul G (2011) Rainfall variability and maize production over the Potohar Plateau of Pakistan. Pakistan Journal of Meteorology 8(15):63–74
Raziei T, Saghafian B, Paulo AA, Pereira LS, Bordi I (2009) Spatial patterns and temporal variability of drought in western Iran. Water Resour Manag 23(3):439
Sajjad H, Ghaffar A (2018) Observed, simulated and projected extreme climate indices over Pakistan in changing climate. Theor Appl Climatol 137(1–2):255–281
Samuelsson P, Jones CG, Willen U, Ullerstig A, Gollvik S, Hansson U, Jansson E, Kjellstro C, Nikulin G, Wyser K (2011) The Rossby Centre regional climate model RCA3: model description and performance. Tellus A: Dynamic Meteorology and Oceanography 63(1):4–23
Schneider U, Becker A, Finger P, Meyer-Christoffer A, Rudolf B, Ziese M (2015) GPCC Full Data Monthly Product Version 7.0 at 0.5°: Monthly Land-Surface Precipitation from Rain-Gauges Built on GTS-Based and Historic Data. https://doi.org/10.5676/DWD_GPCC/FD_M_V7_050
Sen PK (1968) Estimates of the regression coefficient based on Kendall's tau. J Am Stat Assoc 63(324):1379–1389
Shafer BA, Dezman LE (1982) Development of a surface water supply index (SWSI) to assess the severity of drought conditions in snowpack runoff areas. In: Preprints, Western Snow Conference, Reno, NV, Colorado State University, pp 164–175

Smakhtin VU, Schipper EL (2008) Droughts: the impact of semantics and perceptions. Water Policy 10(2):131–143

Syed FS, Yoo JH, Kornich H, Kucharski F (2010) Are intraseasonal summer rainfall events micro monsoon onsets over the western edge of the South-Asian monsoon? Atmos Res 98(2–4):341–346

Tabari H, Abghani H, Hosseinzadeh TP (2012) Temporal trends and spatial characteristics of drought and rainfall in arid and semiarid regions of Iran. Hydrol Process 26(22):3351–3361

Taylor KE (2001) Summarizing multiple aspects of model performance in a single diagram. Journal of Geophysical Research: Atmospheres 106(D7):7183–7192

Tsakiris G, Vangelis H (2005) Establishing a drought index incorporating evapotranspiration. European Water 9(10):3–11

Tsakiris G, Pangalou D, Vangelis H (2007) Regional drought assessment based on the Reconnaissance Drought Index (RDI). Water Resour Manag 21(5):821–833

Ullah K, Shouting G (2012) Moisture transport over the Arabian Sea associated with summer rainfall over Pakistan in 1994 and 2002. Adv Atmos Sci 29(3):501–508

Ullah A, Sun H, Yang X, Zhang X (2017) Drought coping strategies in cotton: increased crop per drop. Plant Biotechnol J 15(3):271–284

Vicente-Serrano SM, Beguería S, López-Moreno JI (2010) A multiscalar drought index sensitive to global warming: the standardized precipitation evapotranspiration index. J Clim 23(7):1696–1718

Wang Z, Yang S, Duan A, Hua W, Ullah K, Liu S (2019) Tibetan plateau heating as a driver of monsoon rainfall variability in Pakistan. Clim Dyn 52(9–10):6121–6130

Wilhite D (2000) Drought preparedness in the U.S. In: Vogt JV, Somma F (eds) Drought and drought mitigation in Europe. Kluwer, The Netherlands, pp 119–132

Willmott CJ, Matsuura K (2005) Advantages of the mean absolute error (MAE) over the root mean square error (RMSE) in assessing average model performance. Clim Res 30(1):79–82

Wu H, Hayes MJ, Weiss A, Hu Q (2001) An evaluation of the standardized precipitation index, the China-Z-index and the statistical Z-score. Int J Climatol 21(6):745–758

Yatagai A, Kamiguchi K, Arakawa O, Hamada A, Yasutomi N, Kitoh A (2012) APHRODITE: constructing a long-term daily gridded precipitation dataset for Asia based on a dense network of rain gauges. Bull Am Meteorol Soc 93(9):1401–1415

Zargar A, Sadiq R, Naser B, Khan FI (2011) A review of drought indices. Environ Rev 19:333–349

Zhang L, Zhou T (2015) Drought over East Asia: a review. J Clim 28(8): 3375–3399

Zhang Q, Gu X, Singh VP, Kong D, Chen X (2015) Spatiotemporal behavior of floods and droughts and their impacts on agriculture in China. Global Planet Change 131:63–72